COMPENSATING FOR THE EFFECTS OF REDUCED SYNCHRONOUS INERTIA ON FREQUENCY STABILITY USING VIRTUAL SYNCHRONOUS GENERATORS

BY

JEFFREY ZHU

THESIS

Submitted in partial fulfillment of the requirements
for the degree of Master of Science in Electrical and Computer Engineering
in the Graduate College of the
University of Illinois at Urbana-Champaign, 2019

Urbana, Illinois

Professor Peter Sauer

Abstract

The power grid has traditionally been dominated by large synchronous generators which have provided frequency stability through their inertia and governor responses. As more renewable energy sources (RES), particularly wind and solar, are added to the grid, they displace synchronous generators. Many of these RES generators do not inherently contribute inertia to the system, so their inclusion in the generation portfolio decreases the aggregate inertia of the grid. Low inertia makes a grid more vulnerable to fast frequency dynamics in the wake of a disturbance. A virtual synchronous generator (VSG) can compensate for the displacement of synchronous generators by emulating the inertia response and governor response of a synchronous generator. This thesis reviews prior investigations into VSGs and then uses a series of simulations to examine how synchronous inertia, VSG sizing, control parameters and battery speed affect the frequency dynamics after a disturbance. The main findings of this thesis are as follows: VSGs have some inherent delay, so a certain amount of synchronous inertia will still be needed even if a VSG is installed. Batteries are an attractive technology to use with VSGs because their fast response times can create VSGs with low delays. A VSG with a faster response offers more benefit to the grid. The best way to control a VSG is to combine strong primary frequency control with inertia control. A VSG that is powerful enough to match the power imbalance caused by a disturbance can stabilize the frequency on its own before governors can typically act, but even a less powerful VSG can benefit the grid by slowing the frequency dynamics following a disturbance.

Acknowledgments

This thesis would not have been possible without the inspiration and support of Professor Sauer. His class in power system dynamics gave me the experience and interest to pursue research into frequency stability. It was his curiosity about renewable energy and batteries on the grid that ultimately inspired this work.

Table of Contents

1. Introduction

For most of the power industry's history, electricity generation has been dominated by large synchronous machines, typically driven by steam or hydro power. Power plants based on these large synchronous generators are known as traditional generators. Over the past couple decades, there has been a worldwide movement to use fewer traditional generation resources and more renewable energy sources (RES), particularly wind and solar power. Although there are renewable resources other than wind and solar (hydro, geothermal, biomass, etc.), their share of the renewable energy portfolio is small and they are not subject to the exponential levels of growth seen by wind and solar [1],[2]. Because of that, this paper, and many others like it, reserve the term *RES* for typical wind and solar generation. A number of important factors lie behind this relatively recent drive towards RES generation. The most well-known reason is environmental. Most traditional generators rely on burning fossil fuels like coal to produce steam which drives the prime mover. Burning fossil fuels release pollutants and greenhouse gases into the environment that have negative impacts on climate and public health [3]. Fossil fuels are also a finite resource. Eventually they will run out, and we need to have alternative energy sources in place before that happens. Luckily, wind and solar resources are abundant and inexhaustible. The amount of solar irradiation reaching the Earth's surface exceeds humanity's power demand many times over. We can use RES generation to extract considerable value from what would otherwise be useless land. The deserts, for instance, are attractive areas to set up solar farms, thanks to their high solar irradiation and low land value. Solar power from the Sahara Desert could meet the electricity demand of Europe, North Africa and the rest of the Mediterranean region [4]. Although RES technology has been around for a while, it has struggled to compete with

traditional generation in the electricity market because of its high capital costs relative to its energy output. However, a combination of advances in technology and government support have made wind and solar increasingly competitive. RES costs have been trending down as technology improves and production expands. Governments have offered support tax benefits, subsidies, research funding and goal setting. Countries all over the world have set ambitious targets for RES "penetration," which is the percentage of demand that is met by renewable generation.

The rising share of wind and solar generation has led to concerns over the frequency stability of the grid. To understand these concerns, we need to understand how the implementation of most wind and solar generators causes them to behave differently on the grid than traditional synchronous generators. Wind turbine generators can be split into two general types: fixed-speed and variable-speed [3],[5]. Most wind turbines connected to the grid are variable-speed turbines [5]. Similarly, solar power is collected in two different ways: photovoltaics (PV) or concentrated solar power (CSP) [4]. Concentrated solar uses the sun's energy to drive a heat engine, similar to most traditional generators. However, most solar power is generated using photovoltaics, which behave very differently from traditional generators. PV arrays are made up of diodes that generate a DC voltage. Since the power grid is an AC system, PV generators cannot be directly connected to the grid. The PV output has to pass through a power converter to be acceptable to the grid. Variable-speed wind turbines have a similar issue. As their name would suggest, variable-speed wind turbines can operate with varying speed, and by extension, varying frequency. The grid cannot accept power whose frequency does not match the grid frequency, so the output of a variable-speed wind turbine has to go through a power converter to synchronize it with the grid. The use of power converters means that variable-speed

wind turbines and PV arrays are electrically decoupled from the grid [6],[5]. Once we see how traditional generators interact with the grid, it will become clear why this decoupling is a challenge to frequency stability.

Synchronous generators are directly coupled to the grid. The frequency of the grid is largely determined by the speed of these generators. The electrical characteristics of the grid directly affect the mechanical behavior of the synchronous generators and vis versa. This relationship is described by the swing equation [7].

$$J\frac{d\omega}{dt} = T_m - T_e \tag{1.1}$$

Here, J is the moment of inertia, ω is the speed of the synchronous generator, T_m is the mechanical torque of the prime mover and T_e is the electrical torque of the generator.

The swing equation can be expressed in terms of either torques or powers. Generally speaking, power engineers prefer to work with power instead of torque. Power is equivalent to torque times angular velocity, so to rewrite the swing equation in terms of powers, multiply both sides of Equation (1.1) by ω. This produces Equation (1.2). Another way to derive Equation (1.2) is to recognize that the difference between mechanical and electrical power is equal to the derivative of rotational kinetic energy with respect to time.

$$J\omega\frac{d\omega}{dt} = P_m - P_e \tag{1.2}$$

Here, P_m is the mechanical power input, which is sustained by whatever energy source is spinning the prime mover. The other power term, P_e, is the electrical power output of the generator which goes out onto the grid.

The swing equation is typically expressed with a term called the inertia constant, denoted by H. It is defined as the kinetic energy of the generator at synchronous speed normalized with respect to its rated power. The inertia constant is measured in seconds and its value represents

the amount of time that the generator can provide its rated power using only its stored kinetic energy.

$$H = \frac{\frac{1}{2}J\omega_s^2}{S_B} \tag{1.3}$$

Equation (1.3) can be rewritten to get an expression for J. Substituting J into Equation (1.2) puts H into the swing equation.

$$\frac{2S_B H}{\omega_s^2}\omega\frac{d\omega}{dt} = P_m - P_e \tag{1.4}$$

The literature often simplifies Equation (1.4) by making the approximation $\omega \approx \omega_s$ [8],[7],[9],[2]. Assuming this approximation allows us to cancel out the speed term, ω.

$$\frac{2S_B H}{\omega_s}\frac{d\omega}{dt} = P_m - P_e \tag{1.5}$$

Equations (1.4) and (1.5) have the speeds in units of r/s and the powers in units of MW. However, it is common practice to write power terms as per unit quantities. This can be done easily to Equation (1.5) by dividing both sides by the base power, S_B.

$$\frac{2H}{\omega_s}\frac{d\omega}{dt} = P_m - P_e \tag{1.6}$$

According to the conservation of power, the power generated must match the power demanded by the load (including transmission losses). Under normal operation, the generation dispatch closely matches the load power demand, but if a generator was suddenly lost while the load remained unchanged then the remaining generators would have to make up the difference by increasing their electrical power output. Unfortunately, the prime movers which provide mechanical power input to the generators cannot change their setpoints fast enough to immediately match the increase in electrical power output. That extra electrical power output still has to come from somewhere. According to the swing equation, when $P_e > P_m$ the generator rotors will decelerate at a rate proportional to the size of the power mismatch. This slowdown indicates

that the generators' rotational kinetic energy is being reduced. When the mechanical input is not enough to supply the electrical output, the difference in power is made up by drawing the generators' rotational kinetic energy. This behavior is known as the inertia or inertial response [8]. Since synchronous generators are directly coupled to the grid, when they lose speed, they reduce the frequency of the grid. This process also works in reverse. If there was a sudden increase in generation or a sudden drop in load, then the frequency of the grid would rise.

Small deviations in frequency caused by generation-load imbalances are acceptable and normal, provided that they are kept under control and not allowed to exceed certain limits. Large drops in frequency and large increases in frequency are both dangerous to the grid, and there are certain measures in place to prevent that from happening. These frequency control schemes cannot immediately react to a generation-load imbalance because they usually rely on changing the mechanical power setpoint of the generators. The inertia has an important role to play here. It buys time for frequency control schemes by resisting changes in speed and frequency. Equation (1.6) shows an inverse relationship between the inertia constant and the rate of change of frequency (ROCOF). Thus, the larger the aggregate inertia of the grid, the easier it is to stabilize the frequency. In a traditional power system largely populated by synchronous machines, the grid has plenty of inertia. However, most wind and solar generators do not inherently contribute inertia to the grid because they are decoupled from the grid by power converters. They are isolated from changes in grid frequency. As more and more of these RES generators are integrated into the grid, they displace traditional generation units and lower the total synchronous inertia of the power system. In places like Germany, which already has high RES penetration, the grid inertia falls to half of what it used to be [1]. Low inertia situations like this are likely to become the norm in many places around the world as renewable energy continues to grow. In

light of that reality, the frequency stability services that were traditionally provided by synchronous generators must be supplemented or found elsewhere.

The rest of this thesis is organized as follows: Chapter 2 reviews the relevant literature. It describes various frequency support mechanisms that have been implemented or proposed. Chapter 2 also introduces the virtual synchronous generator (VSG) as a solution to the problem described in this introduction. It discusses prior work done on the implementation, as well as effects and challenges of VSGs. Chapter 3 reports the simulation of the inertia response for different grid conditions in order to determine how limits on the frequency deviation and ROCOF inform the synchronous inertia and VSG response speed that the grid needs. Chapter 4 reports on the addition of a VSG to the simulation to investigate how the size, control and speed of a VSG affect frequency performance following a disturbance. Finally, Chapter 5 concludes this thesis and summarizes its main findings.

2. Literature Review

The challenges posed by increasing RES generation have not gone unnoticed by industry and academia. Engineers have conducted studies, run simulations, and created devices to improve the frequency stability of the grid. This chapter reviews some of those works and provides context for the following chapters of this thesis. Frequency stability is not a new concern and engineers have developed measures to keep the frequency close to the nominal synchronous frequency, which is 60 Hz in the U.S. When a disturbance upsets the balance between generation and load, it triggers a sequence of responses that arrests the change in frequency and eventually restores the frequency to its nominal value. Section 2.1 describes this sequence step-by-step, summarizing the operating principle of each stage and the role it plays. Section 2.2 describes proposals to use RES generators to provide the frequency support services that have traditionally been provided by the synchronous generators they are displacing. Section 2.3 introduces the concept of the virtual synchronous generator, explaining how it can be used to provide some of the support services described in Section 2.1. Section 2.4 discusses prior research into VSGs, especially those based on energy storage systems. Finally, Section 2.5 surveys the literature to get an idea of how fast a battery energy storage system (BESS) can act, because a VSG supplied by batteries is limited in its ability to respond by the speed of its batteries.

2.1: Overview of Inertia Response and Frequency Control

This problem this thesis seeks to address is the restoration of frequency following a disturbance. To place this work within the proper context, it would be appropriate to understand how the grid responds to a frequency deviation caused by a generation-load imbalance.

In general, the literature divides frequency support into four distinct responses that occur in sequence [1],[3]. The inertia response comes first, immediately after the disturbance. The synchronous generators are electromechanically coupled to the grid, which means that the mechanical speed of the generators is coupled to the electrical frequency of the grid. The inertia response is automatic. It is largely a function of the synchronous generator's mass and cannot be directly controlled. The inertia response dominates the frequency transient for only a brief period. Even though a typical generator has an inertia constant between 2 and 9 seconds [6], the system should never allow its synchronous machines to exhaust all their stored kinetic energy as that would be equivalent to letting the grid frequency run to zero. Usually, another frequency control measure will kick in long before that happens. Another reason not to stay with inertia control for too long is that the inertia response is a physical manifestation of derivative control, since its effect is proportional to the rate of change. It can slow the frequency dynamics, but it cannot stop them.

Primary frequency control (the literature also uses the term "frequency response") kicks in next, typically within 5 to 30 seconds of the disturbance. The delay is there because primary frequency control is the domain of the governors on the generators. It takes time to detect a serious frequency excursion; it takes time for a control action to be calculated and commanded; it takes time for the control action to be executed. All these delays add up. The inherent delay of primary frequency control is actually what gives the inertia response its importance. The inertia response must slow the frequency dynamics enough so that the frequency deviation does not reach dangerous levels before primary frequency control can take effect. Primary frequency control is decentralized proportional control. Each governor acts on its own initiative, without needing a central controller to tell it what to do. The governors increase (in the case of a

frequency drop) the mechanical power setpoint in proportion to the frequency deviation. In order for this to be possible, the generator must be deloaded, meaning that the generator does not operate at its maximum power so that it has room to increase its output. The objective of primary frequency control is to stabilize the frequency.

When the frequency is guided by proportional control, it will settle to a steady-state value with some error. To drive that error to zero, secondary frequency control activates next and introduces an integral control term to the frequency control scheme. Secondary frequency control can last for minutes, and like primary frequency control its action has been mostly automated. If that is not enough to restore the system frequency to its nominal value, then the final recourse is tertiary frequency control. Unlike everything that has come before it, tertiary frequency control is not an automatic or automated response. The operator manually adjusts the generators' power setpoints to restore the frequency. In everyday operation, small random deviations of frequency are common; these are the results of constantly changing loads and generation on the grid. To prevent these insignificant variations from constantly triggering frequency control action, a non-critical dead-band is usually defined about the nominal frequency.

2.2: Frequency Support Options from Converter-Connected RES

When considering the displacement of synchronous generators by converter-connected RES generators, the literature is mostly concerned with compensating for the loss of inertia response and auxiliary services, particularly primary frequency control. The inertia and frequency response are usually coupled with synchronous generators. The inertia response is there by default and the governor is usually built into synchronous generators. A number of researchers have taken the approach that the RES generators themselves should replace the inertia response and primary frequency control they are displacing [10],[5]. This is the approach

that GE took in developing its WindINERTIA and WindCONTROL control products for wind plants [10].

While conventional wisdom says that increasing wind power penetration will degrade the frequency response of the power grid, GE argues that with the appropriate control schemes it is possible for high levels of wind penetration to result in an improved system frequency response. During significant underfrequency events, WindINERTIA temporarily boosts the wind turbine power output for several seconds, similar to how a synchronous generator would boost its power output by drawing on its stored kinetic energy. However, one important difference is that the behavior of WindINERTIA depends on its environmental conditions, namely the wind speed. If the wind speed is low then the power boost has to come from the kinetic energy stored in the wind turbine's moving parts. This kinetic energy must be recovered, and so the period of heightened power output is followed by a period of lowered power output. On the other hand, if the wind speed is high then pitch control can be used to temporarily increase the power captured from the wind. Since the power boost in that case did not come from the stored kinetic energy, there is less need for a following period of underproduction. WindINERTIA does not exactly replicate the inherent response of a synchronous machine. The authors believe that is impractical and unnecessary. The control is asymmetric and only responds to frequency drops. It also only responds to potentially dangerous deviations, in contrast to the inertia of synchronous generators which inherently responds to any deviations. WindCONTROL is designed to emulate the conventional governor response, provided that some active power production is kept in reserve by running the wind plant below its maximum power point. One advantage of WindCONTROL over conventional generators is that a wind plant can typically ramp faster than a thermal generator ("thermal" refers to traditional steam-driven synchronous generators). The authors

make another point about improving the primary response: According to the Western Wind and Integration Study [11], for every 3 MW of additional wind production, there is a 2 MW reduction in thermal unit commitment and a 1 MW reduction in thermal unit dispatch. Thermal units that remain committed but are dispatched to lower power levels continue to contribute to the inertia response and have more headroom to provide a stronger governor response to frequency drops. For the best effect on the frequency response, the inertial and primary control should be combined. Since these are control systems, they can be tuned for optimal performance.

Muljadi et al. [5] reiterated many of the same arguments made by the GE engineers, but he focused on describing the inertia response from different types of wind turbines. In general, constant-speed wind turbines do contribute inertia to the system because they are directly connected to the grid and capable of releasing the kinetic energy stored in their moving parts. In variable-speed wind turbines, the rotating mass is decoupled from the grid frequency by a power converter and so does not inherently produce an inertia response unless controls give it that capability. Variable-speed wind turbines are the dominant type of wind turbine on the grid, which probably explains why the literature typically assumes that increasing wind penetration weakens the system's inherent inertia response. This problem can be handled by providing controls to emulate an inertia response, and such controls are already commercially available. Grid codes and market structures need to be updated so owners of variable-speed wind turbines have an incentive to contribute to frequency stability.

While a wind plant can provide energy for frequency regulation from the kinetic energy of its moving parts, there is no such thing when it comes to PV systems. The typical PV system does not have a large energy buffer; its only native storage is capacitors which do not hold that much energy [6]. PV generation is on the rise and there are significant stability challenges from

integrating large amounts of it to the grid [4]. It used to be the case that PV installations were small and connected at the distribution level, but now there is a trend towards large transmission-scale PV installations. These large PV plants will have a significant impact on the frequency dynamics of the grid. This trend is the result of advances in semiconductor technology and power electronics that had made PV technology more profitable for large-scale energy production. The authors of [4] name a number of issues with the proliferation of PV in the grid, including intermittency, voltage stability and frequency regulation. To cope with these challenges, many countries are updating their grid codes. Other solutions include curtailing PV generation, using energy storage devices, and having dump loads to absorb excess energy.

Dreidy et al. [3] review various inertia response and frequency control techniques for wind and solar RES generators. These generators cannot participate in frequency regulation without the appropriate control scheme. There are two ways this can be done. In the deloading technique, a generator is operated below its maximum power point so as to have some active power in reserve. The other way is to store energy and release it during underfrequency events. Frequency control for a RES can be provided with or without an energy storage system (ESS). The authors consider both cases for wind and solar. Wind turbines without an ESS can still draw on the kinetic energy stored in their rotating parts. How this is done depends on the type of wind turbine. A fixed-speed wind turbine typically has an induction generator connected directly to the grid. Thus, it can provide an actual inertia response but that inertia is usually small compared to that from a traditional generator. A variable-speed wind turbine typically has machines which are decoupled from the grid by a power converter. The converter can be controlled to release the stored kinetic energy in an emulated inertia response. The authors also describe a technique called “fast power reserve” that involves responding to frequency deviations by releasing

constant power for a certain amount of time. The authors describe a one-loop and two-loop frequency control scheme. The one-loop control scheme is simply based on the ROCOF, analogous to the swing equation. Two-loop control has an additional torque input that is proportional to the frequency deviation. Normally, wind turbines are operated at their maximum output power. By shifting the turbine's operating point from its optimal power curve to a reduced power level, a reserve margin can be created for frequency regulation. The authors explain that this can be done by shifting the tip-speed ratio or shifting the blade pitch angle, or some combination of both. The same principle can also be applied to PV systems by shifting the voltage or angle. Since RESs are variable and intermittent, adding an ESS to a generator can increase the reliability of its frequency regulation.

2.3: Frequency Services Provided by a Virtual Synchronous Generator

Traditionally, the inertia in a power grid was taken for granted, despite its importance. With the recent rise in RES generation, attitudes are changing and inertia has been getting attention in the literature. Engineers have been looking at ways to generate a "virtual" inertia response using means other than a synchronous generator. This idea is also called emulated or synthetic inertia [12] because the response is artificially created through controls rather than as a result of actual mass. A VSG is not technically a generator because it is not defined by an ability to convert some other form of energy (kinetic energy, thermal energy, chemical energy, etc.) into electrical energy.

A VSG has three main components: a source of electrical energy, a power converter, and a control scheme. The energy source can be a generator but a popular, and arguably better, idea is to use a battery energy storage system (BESS). Battery systems are usually fast-acting and more flexible than generators. There are also practical problems with using generators to supply

VSGs. RES generators like wind and solar are intermittent, so a VSG supplied by RES generators is not as consistently available as a VSG supplied by batteries. Supplying a VSG with a traditional synchronous generator is practically pointless. The whole purpose of a VSG is to mimic the services that synchronous generators already provide.

Regardless of the energy source, it is the control scheme that makes a VSG what it is. The BESS and power converter simply provide the input and output for the VSG control scheme to act on. A VSG providing synthetic inertia uses a control law based on the swing equation of the synchronous generator. The swing equation can be remodeled as a derivative controller [13],[14],[15],[16],[17],[18] of the form:

$$P_{VSG} = k_d \frac{d\omega}{dt} \tag{2.1}$$

In Equation (2.1), P_{VSG} represents the power output of a VSG unit and ω is the electrical frequency of the grid. Therefore, the constant k_d should be a negative value so that the VSG provides power to the grid in response to falling frequency. In Equation (2.1), all the constants in the swing equation are rolled into a derivative gain constant, k_d. The variables J and ω in Equation (1.2) have no meaning when applied to a BESS-based VSG. A battery system has no moving parts, so it has no moment of inertia and no mechanical speed. A strict Newtonian definition of inertia has the term only apply to those systems that react instantly to oppose acceleration, which is impossible for a controlled system to do. Brogan et al. [12] address this controversy by proposing that emulated/synthetic inertia is that which can replace aspects of synchronous inertia. This echoes the sentiments expressed in [10] that synchronous inertia does not have to be exactly replicated for practical purposes. While the inertia of a synchronous machine is related to its mass in accordance with Newton's first law of motion, the "inertia" of a VSG is arbitrary and mutable [6]. It is not based on anything physical, and it is only limited by

the maximum power of the BESS or the converter. The virtual moment of inertia does not have to represent the actual inertia or energy behind the power converter.

It is also common in the literature to see droop control added to the VSG control law [16],[17],[19],[15].

$$P_{VSG} = k_d \frac{d\omega}{dt} + k_p(\omega - \omega_{ref}) \quad (2.2)$$

This creates a PD controller where $k_p$is the proportional gain and k_d is the derivative gain. A larger proportional gain reduces the frequency deviation and a larger derivative gain smooths the frequency response by damping high-frequency oscillations [20]. According to [15], the derivative gain k_d should be set so that the VSG outputs its maximum power when the maximum ROCOF occurs (independent of the proportional term) and the proportional gain k_p should be set so that the VSG will output its maximum power when the maximum frequency deviation occurs (independent of the derivative term). Increasing $k_p$and k_d will increase the power that is exchanged for the same frequency deviation and ROCOF, respectively.

The inclusion of droop control has significant implications for the potential of a VSG. A VSG whose only job was to emulate inertia would only execute the derivative control. The inclusion of proportional gain enables primary frequency control in a VSG. Since a VSG is a control system, there is no reason why a VSG providing virtual inertia should not also provide primary frequency control [20]. This is a paradigm shift from the traditional view of seeing inertia response and frequency response as two separate services. In a synchronous generator, the inertia response and the frequency response are decoupled. The inertia response is inherent, instantaneous, and uncontrolled while the frequency response is controlled and delayed. The inertia response of a synchronous generator comes from the kinetic energy stored in its rotating mass while its frequency response comes from the governor changing the mechanical power

setpoint. These distinctions do not exist for a VSG. In a VSG, both the inertia response and the frequency response are sourced by the BESS connected behind the converter and they are both regulated by a control scheme. In a synchronous generator, the inertia response comes first, followed by the frequency response some time later. In a VSG, the inertia response and frequency response can come together. When working with VSGs, it makes sense to use inertia emulation and primary frequency control as one combined service in a way that is physically impossible with traditional synchronous generators.

2.4: A Review of Prior Work into VSG Applications

Vassilakis et al. [16] investigated the ability of a BESS to provide primary frequency control as part of a VSG. In the implementation of the VSG model, the main objective of the control is to emulate the inertia and the speed-droop characteristics of a synchronous generator. According to the PD control law, the VSG exchanges power with the grid if the frequency deviates from nominal or there is an acceleration in frequency. Simulation results show that higher penetrations of VSG result in lower frequency deviations caused by sudden load changes. The authors describe a battery charge management strategy which can be summarized as follows: When the frequency deviation exceeds the noncritical window, operate the battery with the VSG control law. When the frequency deviation is within the noncritical window, recharge the battery with a few percent of nominal power (5% or less). The higher the recharge rate, the lower the depth of discharge and the smaller the battery needs to be. The authors found that any charge rate higher than 5% produces little additional improvement.

Tielens and Van Hertem [6] carried out a study on the importance of inertia in power systems. They drew attention to how the increase in dispersed, renewable generation adds stress to the grid because of its intermittent nature, decoupling from the grid, and lack of energy buffer.

They state that the traditional definition of power system inertia, which only considers synchronous inertia, is inadequate for a future power system where many conventional generation units will be displaced by decoupled renewable generation units. Tielens and Hertem redefine system inertia to include synchronous inertia from synchronous generators and virtual inertia from converter-connected generators. The authors note that the converter connected generation already available can be used to deliver a virtual inertia response that compensates for the reduction in synchronous inertia, but they point out two key differences between the synchronous inertia response and the virtual inertia response. The virtual inertia can be manipulated. There are time delays associated with the response of the converter, and time is required to filter the frequency and measure its rate of change. Although these time delays are small, their presence means that the response from a converter will never be as fast as the naturally instantaneous response of a synchronous machine. The paper warns about the risks of a low-inertia system, which manifest in a higher ROCOF and lower nadir (another word for minimum) frequency after a disturbance. Too low a nadir can trigger automatic load shedding, and a higher ROCOF gives governors less time to react before that happens. A high ROCOF can also trip anti-islanding relays. Traditionally, the way many TSOs (transmission system operators) handled this issue was by imposing operational limits on the penetration level of converter-connected generation. That is a stop-gap measure and not a good long-term solution if RES generation continues to grow, so TSO's have two other options they can use to cope with a system that has a high penetration of converter-connected generation. One approach is to adapt the power system's equipment, grid codes and protection to cope with larger a ROCOF and frequency swings. The other is to provide virtual inertia or build generators with higher synchronous inertia. The solution might be a combination of both approaches.

Ulbrig et al. [1],[2] address the impact of low rotational inertia on the power system as well as how to compensate for its decline. One of their insights is that frequency stability analysis often assumes that the inertia constant is the same for all swing equations of a multi-area system. That assumption may have been valid in the past, but it is increasingly no longer the case. Instead of using a global inertia constant, we have to start using individual inertia constants for each grid area depending on how much converter-connected generation versus conventional generation is dispatched. Overall, as the pool of conventional power plants diminishes, bringing down the level of rotational inertia, the frequency dynamics will be faster. With faster frequency dynamics, there is a question of whether the primary frequency control will be fast enough to act before a critical frequency drop can happen. Faster frequency dynamics also amplify the transient power over tie-lines, and if those get too large or too fast then they can trip short-circuit relays, further aggravating the situation. One option to mitigate the impact of low inertia is to use a primary frequency control that deploys faster. Another option is to provide synthetic inertia through PV and wind generators or with storage. BESS units are well-suited to provide synthetic inertia and primary frequency control because of their fast response.

Bevrani and Raisch [13] described the dangers of serious frequency deviations and looked at how VSGs can help the grid have a large share of distributed RES generation without compromising its stability. They describe a VSG concept comprised of an energy source, an inverter and a control based on the swing equation. The motivation for their work is concern that abnormal frequency deviations can threaten the grid by damaging equipment, degrading load performance, overloading transmission lines and triggering protection devices. Under normal operation, small frequency deviations can be automatically attenuated by primary frequency control. For larger frequency deviations, secondary control, also known as load frequency

control (LFC), assumes responsibility for restoring the system frequency. More serious disturbances may result in rapid frequency changes that LFC cannot cope with. In that case, additional measures may need to be taken such as deploying tertiary control, standby supplies, or underfrequency load-shedding (UFLS). The authors also discuss demand-side frequency control, in which users can contribute to frequency control through frequency-sensitive loads such as induction machines and frequency-sensitive relays. The demand-response is usually not taken into account when calculating the overall frequency response, but that may be a missed opportunity because incorporating demand response into frequency control can decrease the required generation-side contribution to frequency response.

Torres and Lopes [14] consider applying an ESS-based VSG to serve the frequency stability needs of an autonomous wind-diesel power system. They are interested in autonomous wind-diesel systems in particular because of their viability for small isolated grids. Small grids are more vulnerable to disturbances and fluctuations because they have less inertia and fewer resources. In their work, they study a system comprised of two diesel generators and a wind turbine. To provide virtual inertia support they add an energy storage device connected to the bus through a two-way converter. When the load is high, both diesel generators are operating, so the power contribution of the wind turbine is relatively small. Since the wind penetration is low, the frequency variations caused by fluctuations in wind are small. When the load is high, only one diesel generator is dispatched, which means the wind penetration is high. This demonstrates the utility of having additional frequency support services during low-load conditions. The authors describe a frequency control strategy that involves the diesel generator speed governor and the VSG control algorithm working in concert. The virtual inertia control is a derivative controller based on the swing equation. The system inertia is the sum of the synchronous moment of inertia

and the virtual inertia gain. Their simulation results show that adding virtual inertia decreases the natural frequency and damping ratio, which makes the system dynamics slower and more oscillatory. They also find a direct relationship between the virtual inertia gain and the ESS power flow. Adding virtual inertia reduces the maximum deviation in rotor speed following a disturbance. In their experiments, they model the ESS as an ideal component with no bounds on power flow or capacity, but they propose that parameters such as the maximum charging/discharging capacity and power can be derived from the VSG power profile. In a separate paper, de Haan and Visscher [21] propose the following method of sizing the VSG parameters: The minimum VSG storage size should be proportional to the virtual inertia times the maximum allowable frequency deviation, and the maximum virtual inertia should be proportional to the VSG's nominal power divided by the maximum allowable ROCOF.

Oudalov et al. [22] developed a set of rules to optimize a BESS for primary frequency control. The motivation for their study was an earlier work [23] which examined the range of applications that a battery storage can serve and determined that the application with the highest value is providing primary control reserve. When the authors say "optimize" they mean minimizing the BESS capacity while still meeting the requirements for frequency control. The cost of a BESS is directly related to its capacity. The authors observed that most BESS units tested for frequency regulation were overdimensioned, making them too expensive to be economically practical. First, they surveyed four different types of batteries and found that lead-acid was the cheapest and therefore the most economical solution. Outside of this particular article, there are examples in the literature for using lithium-ion batteries [12],[20], so there is not a clear consensus as to which storage technology is the best. The authors of [22] offer a set of operating rules that minimize the required BESS capacity. The general idea is to keep the

battery's state-of-charge (SOC) within certain limits when there is not a disturbance by charging/discharging at low power, then charging/discharging the battery at high power in response to a disturbance. They include emergency resistors to act as dump loads in case the batteries become fully charged and excess energy still needs to be dissipated. Without emergency resistors, the batteries would have to be large enough to absorb the worst-case overfrequency disturbance.

Alhejaj and Gonzales-Longatt [24] investigated the use of grid-scale BESS to provide an inertia response. They used simulations to verify that a BESS can improve the system's frequency response. Fast-fired gas turbines traditionally have been used to provide an active power reserve for frequency stability, but recent advances in battery technology, along with falling prices, may allow BESSs to replace gas turbines in that role. A BESS can provide better virtual inertia support than a variable-speed wind turbine because the virtual inertia constant of a BESS is controllable whereas that of a variable-speed wind turbine is variable and restricted by operational limitations. They found that increasing the virtual inertia constant improved the inertia response and provided better frequency support. However, a high inertia constant makes the BESS discharge faster. If the BESS discharges too quickly and runs out of charge early, then the power injection could suddenly cut out and create a new frequency disturbance. Also, if the size of the disturbance is too high then the BESS might run out of charge before the frequency can be restored. Finally, they looked at how system robustness impacts BESS performance. The system robustness is represented by the total equivalent transmission impedance X_L. They found that if X_L was low then the BESS inertia response could provide effective frequency support. As X_L increases, the frequency and SOC drop further. This result demonstrates that the BESS's location on the transmission system impacts its performance.

Moon et al. [17] studied the use of a BESS for primary frequency control in South Korea. This application of ESS has been demonstrated in other countries [25] and South Korea has already installed hundreds of megawatts of BESS capacity for frequency control. They modeled a system with a gas, hydro, steam turbine and BESS. In simulation, they looked at the peak time case where the power system is large and the off-peak time case where the power system is smaller. Comparing the two cases, they found that a BESS providing primary frequency control is more impactful during the off-peak times when the system's size is smaller. In both cases, they found that when BESS primary reserves displace steam turbine reserves, the nadir frequency improves because the steam turbine's response is slow and the BESS's response is fast. Another reason is that when a conventional generator provides primary frequency control, it is typically deloaded by 5% of its rated power. A BESS, on the other hand, can be used with its full rated power.

The virtual inertia is malleable, and that is the basis for the basis for a flexible VSG control algorithm proposed by Alipoor et al. [26]. They describe a VSG with an alternating moment of inertia that effectively damps transient oscillations. In the alternating inertia control scheme, the virtual moment of inertia is changed according to the frequency ω and its rate of change $d\omega/dt$. During an oscillation, the sign of $d\omega/dt$ together with the sign of the frequency deviation $\Delta\omega$ indicates whether the system is accelerating or decelerating. If both signs are the same then the frequency is accelerating; if the signs are opposite then it is decelerating. The objective is to quickly damp the frequency oscillations by reducing the acceleration and boosting the deceleration. The ROCOF determines the rate of acceleration/deceleration. The swing equation shows how $d\omega/dt$ is inversely related to the moment of inertia J. It follows that J should be large during periods of acceleration to reduce the acceleration and J should be small during

periods of deceleration to boost the deceleration. By varying the moment of inertia in each half cycle, a damping effect is imposed on the transient energy, proportional to the difference in the values of *J*. This control scheme achieves rapid decay of transient energy and improves stability compared to a SG or a VSG with fixed inertia. Alipoor et al.'s simulations show that a VSG with alternating inertia control can stabilize a disturbance that a VSG with fixed inertia cannot.

2.5: Investigation into the Speed of a BESS

There is some delay associated with a BESS-based VSG. This delay can affect the frequency dynamics, so it is natural to ask how fast a BESS can respond and whether it is fast enough to meet the needs of the system. The following sources presented in this section offer some potential answers, but it will quickly become obvious that there is a lack of consensus on a specific response time. However, there is at least a general consensus that a BESS can respond in under a second. Within that one second window, there is considerable variation in numbers presented by the literature. There is at least a strong consensus in the literature that a BESS is fast enough to provide frequency support services, which includes inertia emulation and primary frequency control.

Comparing BESS times across the literature is not as straightforward as it may seem because there is no standard way of reporting a BESS's speed. Some sources list just a single number and call it the "response time" [27],[28]. Other sources use two numbers: a delay time and a ramp time [12],[29]. Finally, there are some sources that model the BESS's reaction with a time constant [30],[31],[32].

A table in [27] lists the response time of a BESS at 30 ms, which is fast but slower than the 5 ms listed for SMES, flywheels and supercapacitors. The number from that table is used in [17] to extrapolate a battery response model with a simple first-order time delay function of 0.03 s.

In 1988 a 10 MVA converter was put into service to connect an energy storage system to the grid. According to Walker [30], the converter was able to provide a rapid power response with a 16 ms time constant to changes in power command. Senjyu et al. [31] assumed a battery time constant of 0.1 s in their models. Kottick et al. [32] used a time constant of 0.5 s in studying the effects of a 30 MW battery in regulating the isolated Israeli power system. However, the authors of the Israeli study say that the time constants can range from a few milliseconds to a second. That is fast enough to make a BESS useful for the frequency regulation of an island power system. BESS facilities can reduce both frequency fluctuations and the inertia response required from synchronous generators. Through simulations, they verified that a BESS facility reduces frequency deviations caused by sudden load changes.

Greenwood et al. [28] showed that an ESS with a response time of 80 ms is fast enough to provide an enhanced frequency response (EFR) service. EFR is a service designed to be delivered by ESSs and to be much faster than traditional primary frequency control. Delille et al. [33] describe something similar that they call “dynamic frequency control support.” The basic idea is to use the short response time of distributed energy storage systems to inject power within milliseconds or a second after a loss of generation. During the subsequent frequency fall, some power is supplied by the BESS instead of being drawn from the kinetic energy of the rotating masses. The storage thus behaves as virtual inertia by helping reduce the ROCOF both before and during the activation of primary frequency control.

Brogan et al. [12] studied how the delay time, ramp time and BESS power affect the nadir frequency and ROCOF following a sudden loss of generation or increase in load. They base their response model of a delay time and ramp time on the actual response of the 10 MW BESS at Kilroot power station. The delay time is how long it takes for the BESS to start supplying power after a disturbance. The delay time is mainly set by how long it takes for the frequency to drop below the controller's frequency dead-band. The rampup is linear because the BESS at Kilroot mainly implements proportional control. Consequently, the BESS output rises linearly as the frequency falls. The ramp time is mainly restricted by the technology or by grid considerations. The authors argue that the speed of BESS suits it well to providing power between the activation of the inertia response and the activation of frequency response. They simulated a grid that loses about 10% of its generation and was supported by a BESS on one bus. Using their grid model, they determined how fast a BESS needed to be in order to render effective services. For the BESS to have a significant effect on improving the nadir frequency, the sum of its delay time and ramp time must be less than the time to the nadir frequency. In other words, the BESS needs to be fully powered up before the nadir frequency is reached. The authors found that, for their system, a combined delay and ramp time of 0.52 s is enough to provide the maximum reduction in frequency drop. The impact of delay time on performance is twice that of ramp time. A slower delay and ramp time can be compensated by increasing the BESS power. However, there are limits to how much the delay time, ramp time and power output could be improved before further improvements see diminishing returns. One reason has to do with the fact that the frequency nadir is largely determined by how much energy is delivered to the system before it reaches the nadir. If, for example, the frequency nadir occurs 5 s after the disturbance, then reducing the combined delay and ramp time from 2 s to 1 s does not

double the energy delivered. A second source of diminishing returns on improving the nadir is that the BESS's efforts reduce both the time to frequency nadir and the frequency deviation. These are desirable outcomes, but they simultaneously make the BESS less effective. Reducing the time to frequency nadir reduces the time available for the BESS to deliver energy. Reducing the frequency deviation weakens the primary frequency control. Finding the optimal parameters for ROCOF service is complicated by the fact that the ROCOF has to be estimated and the estimation affects the performance. Despite that, the authors claim that ROCOF reduction is a BESS's most valuable service because it is the first service that a BESS can provide after a fault and it complements the services that follow. Based on the method used in this study, a BESS needs to have a delay time of less than 200 ms and a response time of less than 750 ms to qualify for ROCOF service, with optimal performance reached as the delay time approached 150 ms and the ramp time approached 300 ms. Most BESS technologies available today should be able to meet those requirements [34]. For example, the lithium-ion batteries at Kilroot can respond in under 30 ms and ramp to full power in 100 ms.

Echoing the sentiments of the previous article, [29] contends that synthetic inertia devices must deliver power during the maximum ROCOF, which they observe to occur within 500 ms of the fault. Since the delay time has a significant effect on synthetic inertia performance, the authors study how to reduce that time by rapidly detecting underfrequency events through monitoring synchronous machines. The delay time mainly comes from the time needed to detect and categorize the frequency transient. Ideally, that happens in milliseconds, but Brogan et al. [29] admit that their method needs refinement. They do not look at improving the ramp time because that is constrained by the technology rather than the control algorithm.

3. Time-of-Support and Frequency Constraints on a System with Synchronous Inertia

As governments around the world set ambitious targets for RES penetration, an important question to ask is how high the penetration level can go without compromising the stability of the power grid or degrading its performance. The reason why increased levels of RES threaten stability is that they displace synchronous generators and the support services they provide. Therefore, a good place to start answering this question would be to study how much synchronous generation must be kept on hand. There are many ways that synchronous generators support the grid, but this study will focus on how much synchronous inertia is required. Even with the presence of VSGs, at least some level of conventional synchronous generation should be kept on hand. For one thing, conventional generation is not held hostage to the intermittent and inconsistent behavior of wind and solar generation, so the integration of conventional generation can help lessen the disturbances that can be triggered by sudden changes in wind or solar irradiation for a system with a large amount of RES penetration.

Another concern comes from the fact that a BESS-based VSG has a nonzero response time. More generally, the same can be said for any controlled system. There will always be some time spent in taking input measurements, propagating signals, filtering the results, computing the control output and waiting for the response. The total time taken varies depending on the technology and technique, but based on findings from the literature review, a reasonable range for the reaction time of a BESS would be between 5 ms and one second. No doubt a BESS-based VSG is fast, but there will always be a period of time right after a disturbance, and before the VSG can act, when the synchronous inertia must stand alone. The synchronous inertia is not a controlled system, so it has none of the aforementioned time sacrifices. If there is not enough synchronous inertia in the system, then it is entirely possible for the frequency dynamics

following a disturbance to degrade the system before the virtual inertial response has a chance to kick in. That concern is the motivation for this chapter. Section 3.1 describes the simulation model and its intended purpose. Section 3.2 investigates how "time-of-support" and frequency constraints relate to restrictions on the inertia constant and the disturbance size.

Here, *time-of-support* refers to the time following a disturbance to avoid reaching frequency constraints that would degrade the system. The frequency constraints considered here come in two flavors. The first is the under-frequency load shedding (UFLS) limit, which imposes limits on how low the frequency should go. UFLS is intended to protect the grid frequency by addressing the frequency drop at its source, which is the electric power demand exceeding the mechanical power supply, by disconnecting load. While this does fix the problem, it greatly inconveniences the customers who are disconnected so it is normally considered an emergency measure and something to be avoided. The second frequency constraint is on the rate of change. Anti-islanding relays are so named because they are intended to be triggered by the high ROCOF that can result from islanding. But therein lies the problem. Anti-islanding relays are triggered not only by islanding, but by whatever creates frequency dynamics with high ROCOF. The time-of-support is largely a function of UFLS. That's because the highest ROCOF tends to occur immediately after the disturbance. Time-of-support is relevant if the initial ROCOF is low enough that relays do not immediately get triggered. UFLS becomes a greater concern over the course of time as the frequency continues to fall.

3.1: Setup of the Experiment

The objective was to simulate the short-term frequency response following a disturbance due to the synchronous inertia in order to visualize the appropriate time-of-support given a certain set of conditions. The frequency response was evaluated across a typical range of inertia

constants. One of the reasons why the inertia constant H is preferred over the moment of inertia J is that the value of J can vary greatly across machines while H values typically fit within a consistent range of about 2 to 10 [35]. The results of this chapter will provide the context to understand later experiments in Chapter 4 that study VSG implementation.

A power grid is a complicated system, with many different parts that are constantly changing. Modelling it accurately is a tremendous undertaking in and of itself and involves parameters that are beyond the scope of this discussion. Therefore, some simplifications and abstractions are made for this experiment model. In the real grid, loads are highly diverse and variable; their characteristics can be modeled as a combination of constant impedance, constant current and constant power behavior. However, since frequency dynamics are primarily concerned with the consequences of power imbalances, all the load of this test system is condensed into a constant power load. Likewise, there are many different types of generators, each with its own characteristics, but it is the dynamics of synchronous generators that is the concern of this experiment and so the test system's generation is modeled by a single synchronous generator. The transmission lines are considered to be ideal. Before the disturbance, the load draws 1 p.u. of real power from the generator at unity power factor; the generator operates in steady-state at a synchronous speed of 60 Hz. The simulation is allowed to run in steady-state for one second before a disturbance is imposed on the system. The disturbances are modeled as step increases in the load power demand, which in practical terms can mean that a new load has been connected or that some generation was lost. In this thesis, the size of the disturbance is measured as a percentage of the original load. A 20% disturbance, for example, means that the load changed by 20% from 1 p.u. to 1.2 p.u.

There are many different ways to model a synchronous machine, including those that model the rotor angle and voltage dynamics. However, here the load is considered to be a constant real power load and reactances are ignored; the rotor angle and voltage dynamics are neglected in order to focus attention on the frequency dynamics governed by the swing equation and minimize interference from other parameters. Rather than trying to model a specific motor, this simulation model aims to be as general as possible in order to generate results that can approximately apply to any generic machine or an aggregate of machines.

$$\frac{2H}{\omega_s}\frac{d\omega}{dt} = P_m - P_e \tag{3.1}$$

To record the frequency dynamics in MATLAB, numerical integration by Euler's method was applied to Equation (3.1).

$$\omega(t + \Delta t) = \omega(t) + \frac{\omega_s}{2H}(P_m - P_e) * \Delta t \tag{3.2}$$

The frequency at each timestep was recorded and used to produce the figures and tables displayed in Section 3.2.

The governor and turbine controls are deliberately not modeled in this chapter. This is done because the simulation time scale is short, on the order of seconds and milliseconds, and the initial frequency dynamics following a disturbance are dominated by the inertial response [5]. The governor response is generally provided at a much later time on the order of seconds to tens of seconds [10]. Thus, by omitting the governor and turbine dynamics, the simulation will better express the frequency dynamics before the activation of primary frequency control, which is the target time scale for a BESS-based VSG to act. As a consequence, the mechanical power output of the synchronous generator remains constant over the time ranges of this chapter's simulations.

3.2: Simulation Results and Analysis

Figures 3.1 and 3.2 display the simulated synchronous inertial response due to a step change in load power at one second. Figure 3.1 illustrates how increasing the inertia constant reduces the frequency deviation. The difference is especially pronounced at lower inertia values. The difference in frequency deviation between H=2 and H=3 is much larger than the difference in frequency deviation between H=9 and H=10. This is important to keep in mind as the synchronous inertia of power grids continues to fall. Each successive decrease in inertia will have a larger impact on the frequency nadir than the one before. Figure 3.2 displays how larger magnitudes of disturbances produce correspondingly larger magnitudes of frequency deviation. It also shows that additions in load lead to falling frequency while reductions in load lead to increasing frequency, assuming the generation stays constant.

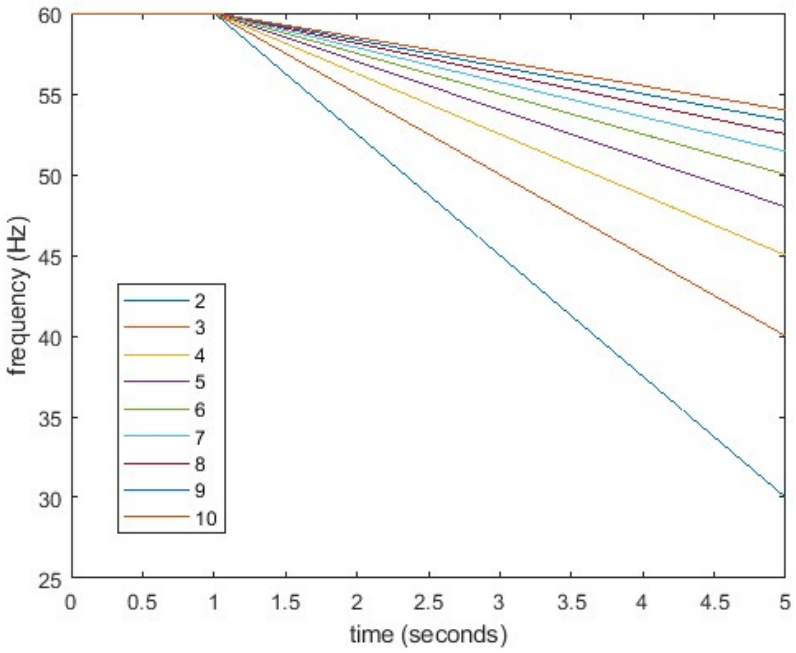

Figure 3.1: The inertia response following a 50% disturbance at time = 1 s for various inertia constants.

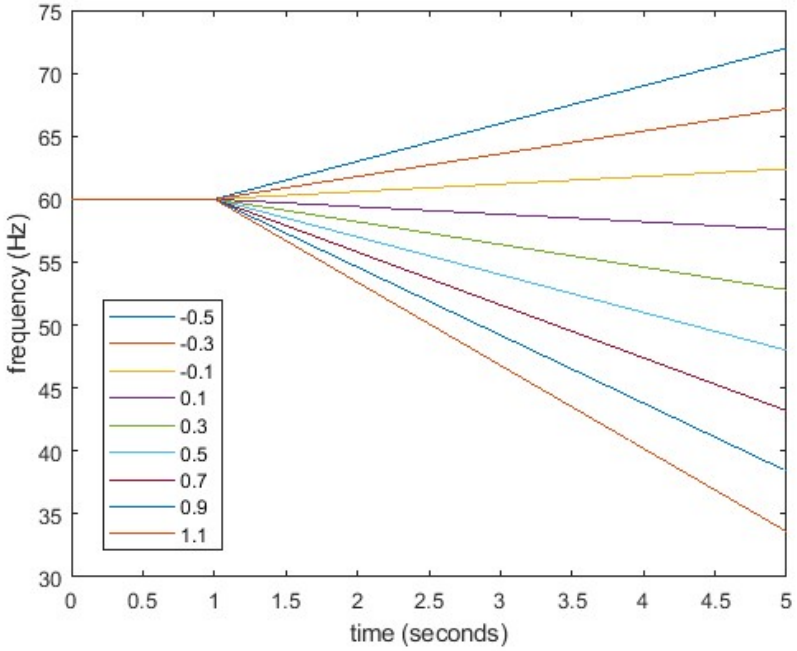

Figure 3.2: The inertia response for various disturbance sizes at time = 1 s with an inertia constant of 5. The load starts at 1 p.u. The legend shows the change in load, in terms of p.u., due to the disturbance.

Using the aforementioned simulation setup, four data tables were generated that take snapshots of the frequency at different times following a disturbance. At each time stamp, the frequency is tabulated based on the size of the disturbance and the value of the inertia constant. The disturbances range from a step increase of 5 to 50% in increments of 5. The range of inertia constants is chosen to be the typical range of 2-10, so as to show what behavior can be anticipated from realistic inertia levels. To give some context to what these numbers can mean, [1] describes an inertia constant of about 6 as typical for the German power grid, with periods of high RES dispatch causing the inertia constant to drop as low as 3-4. Based on that, inertia constants greater than 5 may be interpreted as representing a conventional power grid dominated by synchronous generation, while inertia constants below 5 may represent a future grid with high RES penetration.

Table 3.1: The frequency 5 s after a disturbance for various inertia constants and disturbance sizes.

	Inertia constant (s)									
Disturbance ΔP(p.u.)		2	3	4	5	6	7	8	9	10
	.05	56.25	57.50	58.12	58.50	58.75	58.92	59.06	59.17	59.25
	.10	52.50	55.00	56.25	57.00	57.50	57.85	58.12	58.33	58.50
	.15	48.75	52.50	54.37	55.50	56.25	56.78	57.18	57.50	57.75
	.20	45.00	50.00	52.50	54.00	55.00	55.71	56.25	56.66	57.00
	.25	41.25	47.50	50.62	52.50	53.75	54.64	55.31	55.83	56.25
	.30	37.50	45.00	48.75	51.00	52.50	53.57	54.37	55.00	55.50
	.35	33.75	42.50	46.87	49.50	51.25	52.50	53.43	54.16	54.75
	.40	30.00	40.00	45.00	48.00	50.00	51.42	52.50	53.33	54.00
	.45	26.25	37.50	43.12	46.50	48.75	50.36	51.56	52.50	53.25
	.50	22.50	35.00	41.25	45.00	47.50	49.28	50.62	51.66	52.50

Table 3.2: The frequency 1 s after a disturbance for various inertia constants and disturbance sizes.

	Inertia constant (s)									
Disturbance ΔP(p.u.)		2	3	4	5	6	7	8	9	10
	.05	59.25	59.50	59.62	59.70	59.75	59.78	59.81	59.83	59.85
	.10	58.50	59.00	59.25	59.40	59.50	59.57	59.62	59.66	59.70
	.15	57.75	58.50	58.87	59.10	59.25	59.35	59.43	59.50	59.55
	.20	57.00	58.00	58.50	58.80	59.00	59.14	59.25	59.33	59.40
	.25	56.25	57.50	58.12	58.50	58.75	58.92	59.06	59.16	59.25
	.30	55.50	57.00	57.75	58.20	58.50	58.71	58.87	59.00	59.10
	.35	54.75	56.60	57.37	57.90	58.25	58.50	58.68	58.83	58.95
	.40	54.00	55.50	57.00	57.30	58.00	58.28	58.50	58.66	58.80
	.45	53.25	55.50	56.62	57.30	57.75	58.07	58.31	58.50	58.65
	.50	52.50	55.00	56.25	57.00	57.50	57.85	58.12	58.33	58.50

Table 3.3: The frequency 500 ms after a disturbance for various inertia constants and disturbance sizes.

	Inertia constant (s)									
Disturbance ΔP(pu)		2	3	4	5	6	7	8	9	10
	.05	59.62	59.75	59.81	59.85	59.87	59.89	59.90	59.91	59.92
	.10	59.25	59.50	59.62	59.70	59.75	59.78	59.81	59.83	59.85
	.15	58.87	59.25	59.43	59.55	59.62	59.67	59.71	59.75	59.77
	.20	58.50	59.00	59.25	59.40	59.50	59.57	59.62	59.67	59.70
	.25	58.12	58.75	59.06	59.25	59.37	59.46	59.53	59.58	59.62
	.30	57.75	58.50	58.87	59.10	59.25	59.35	59.43	59.50	59.55
	.35	57.37	58.25	58.68	58.95	59.12	59.25	59.34	59.41	59.47
	.40	57.00	58.00	58.50	58.80	59.00	59.14	59.25	59.33	59.40
	.45	56.62	57.75	58.31	58.65	58.87	59.03	59.15	59.25	59.32
	.50	56.25	57.50	58.12	58.50	58.75	58.92	59.06	59.17	59.25

Table 3.4: The frequency 100 ms after a disturbance for various inertia constants and disturbance sizes.

	Inertia constant (s)									
Disturbance ΔP(p.u.)		2	3	4	5	6	7	8	9	10
	.05	59.92	59.95	59.96	59.97	59.975	59.978	59.981	59.983	59.985
	.10	59.85	59.90	59.92	59.94	59.950	59.957	59.962	59.967	59.970
	.15	59.77	59.85	59.88	59.91	59.920	59.936	59.944	59.950	59.955
	.20	59.70	59.80	59.85	59.88	59.900	59.914	59.925	59.933	59.940
	.25	59.62	59.75	59.81	59.85	59.875	59.893	59.906	59.917	59.925
	.30	59.55	59.70	59.77	59.82	59.850	59.871	59.888	59.900	59.910
	.35	59.47	59.65	59.73	59.79	59.825	59.850	59.869	59.883	59.895
	.40	59.40	59.60	59.70	59.76	59.800	59.829	59.850	59.867	59.880
	.45	59.32	59.55	59.66	59.73	59.775	59.807	59.831	59.850	59.865
	.50	59.25	59.50	59.62	59.70	59.750	59.786	59.812	59.833	59.850

The cells of Tables 3.1-3.4 are color coded to highlight the UFLS settings. Sources differ on what exactly the boundary is, but the two numbers that often come up are 59.5 Hz [2],[36],[37] and 59.3 Hz [38],[39],[40]. Based on that information, frequencies below 59.3 Hz are highlighted in red, frequencies between 59.3 Hz and 59.5 Hz are in yellow, and frequencies above 59.5 Hz are in green. The way to interpret the tables is to see red as guaranteed UFLS, yellow as possible UFLS, and green as safe.

Table 3.1 depicts the frequency 5 s after the disturbance. This time was chosen to test because primary frequency control can have a maximum delay time of 5 s and fully activates by 30 s [2]. But if the results in Table 3.1 are anything to go by, 5 s is too long to wait for anything other than a rather small disturbance. Given any disturbance greater than 5% for typical inertia constants, the frequency will fall below ULFS threshold at 5 s, assuming of course that no control action has been activated. In transient simulation studies of power grids, it is standard to have the tested disturbance be the loss of the largest generation unit on the grid. This can be a problem for small island grids with few generation units where the loss of a single generator represents a much larger disturbance than for a continental-sized grid. Case in point [12]: In 2016 the Irish power system had a generator trip that was supplying 430 MW to the grid, which

represented a 10.5% power imbalance. Luckily for most of us, national or continental size grids are in the range of tens if not hundreds of GW, so even the disturbance caused by the loss of a large generator is typically on the order of 1% of its size [17],[2],[10]. Also, the bigger the grid, the more synchronous machines it will have coupled, so the bigger its inertia. The exact inertia constant of a grid is actually quite challenging to estimate; [6] points out a number of technical hurdles that complicate grid inertia measurement. Also, the system inertia is highly variable as it depends on the size of the grid, the composition of generation resources, the nature of the load, the level of demand (which varies over time) and the power dispatch solution. The result is that estimates of system inertia constants can vary wildly, even for the same grid, so there is not really a "typical" inertia constant for a power grid as there is for synchronous machines. A reasonable range could be 3-9 based on the German power grid [1] and the UK power grid [41].

Table 3.2 samples the frequency 1 s after the disturbance. The UK's Enhanced Frequency Response (EFR) service, which is intended for energy storage systems, requires a response time within one second [28]. It is generally agreed that a BESS can act in under a second. Most governor time constants are larger than a second. Therefore, one second can be seen as the boundary between the response of a slow BESS and a fast governor/droop response. The results in Table 3.2 show that for disturbances below 10-15% with inertia constants higher than 6, UFLS can be avoided one second after the disturbance. This might be achievable with the current grid, but as more RESs are integrated into the grid the inertia will decrease and the volatility of wind and solar will add to the risk of large and sudden disturbances. The net effect is to risk moving the grid into the "red zone" of Table 3.2.

Table 3.3 and Table 3.4 show the frequency 500 ms and 100 ms following the disturbance, respectively. Based on the numbers seen in the literature review, this represents the

time scales within which a BESS can reasonably be expected to react. If the BESS can act even faster than 100 ms, as some sources claim, then UFLS can be avoided even for disturbances as large as 50% with inertia constants as low as 2 or 3. These tables illustrate the significant positive impact that the shorter response time of a BESS, compared to the relatively slower primary frequency control, can have on the evolution of frequency after a disturbance.

Table 3.5 depicts the ROCOF that results from disturbances at various levels of inertia. With only the swing dynamics modeled, the ROCOF does not vary with time, so only one table is necessary. Table 3.5 is color coded according to the trigger level for anti-islanding relays, which can be between 0.5 and 1.0 Hz/s [29]. Based on these numbers, red is used to represent guaranteed tripping (ROCOF>1), yellow represents the range of possible tripping (between 0.5 and 1.0), and green represents a safe ROCOF. Comparing Table 3.5 with the previous four tables it can be seen that, for time scales longer than a second, the frequency dynamics are mainly constrained by the UFLS settings. For time scales under a second it can be seen that the frequency dynamics are mainly constrained by the their ROCOF limit. From this comparison and observation, it is logical to conclude that within the time scale that a BESS should provide frequency support there must still be sufficient synchronous inertia to damp the ROCOF in the immediate aftermath of a disturbance so that anti-islanding relays are not triggered before virtual inertia can make its contribution. However, it is easy to see that the “green zone” in Table 3.5 is not very large, even with higher inertia constants, so it might be a good idea to raise the ROCOF tolerance of anti-islanding relays. If the ROCOF tolerance range started at 1 Hz/s instead of 0.5 Hz/s, Table 3.5’s “green zone” would more than double.

Table 3.5: The ROCOF after a disturbance for various inertia constants and disturbance sizes.

	Inertia constant (s)									
Disturbance ΔP(p.u.)		2	3	4	5	6	7	8	9	10
	.05	0.750	0.500	0.375	0.30	0.25	0.214	0.188	0.167	0.150
	.10	1.500	1.000	0.600	0.60	0.50	0.429	0.375	0.333	0.300
	.15	2.250	1.500	1.125	0.90	0.75	0.643	0.563	0.500	0.450
	.20	3.000	2.000	1.500	1.20	1.00	0.857	0.750	0.667	0.600
	.25	3.750	2.500	1.875	1.50	1.25	1.071	0.938	0.833	0.750
	.30	4.500	3.000	2.250	1.80	1.50	1.286	1.125	1.000	0.900
	.35	5.250	3.500	2.625	2.10	1.75	1.500	1.323	1.167	1.050
	.40	6.000	4.000	3.000	2.40	2.00	1.714	1.500	1.333	1.200
	.45	6.750	4.500	3.375	2.70	2.25	1.929	1.688	1.500	1.350
	.50	7.500	5.000	3.750	3.00	2.50	2.123	1.875	1.667	1.500

By manipulating Equation (3.1), it is possible to directly calculate the minimum synchronous inertia for a given UFLS setting. The derivation is shown below in Equations (3.3) - (3.5).

$$\int_{\omega 1}^{\omega 2} d\omega = \int_{t1}^{t2} \frac{(P_m - P_e)\omega_s}{2H} dt \tag{3.3}$$

$$\Delta\omega = \frac{\Delta P \omega_s}{2H} \Delta t \tag{3.4}$$

$$H_{min} = \frac{\Delta P \omega_s \Delta t}{2\Delta\omega_{max}} \tag{3.5}$$

Here, ΔP is the magnitude of the disturbance in per unit, ΔT is the time after the disturbance, and $\Delta\omega_{max}$ is the maximum frequency deviation. Example results are shown in Table 3.6 for a UFLS setting of 59.3 Hz. One thing to keep in mind is that there is usually not just one hard limit for the UFLS. Rather, it is common for there to be multiple successive levels of UFLS. For example, ERCOT specifies three UFLS thresholds [39]: At 59.3 Hz, 5% of the load is shed. At 58.9 Hz, 15% of the load is shed. Finally, at 58.5 Hz, 25% of the load is shed. Rather than being simply an on-off switch, UFLS is a multi-stage process. If some load shedding can be considered acceptable, then the H_{min} may be lower than what is depicted in Table 3.6. The aforementioned ERCOT limits are not universal and it is possible to find other UFLS settings

proposed in the literature [38]. For these reasons, Table 3.6 is presented as a viable example rather than a universal design reference. The table is color coded so that atypically high inertia constants (H>10) are in red, typical inertia constants are in green and very low inertia constants are in blue.

Table 3.6: The minimum synchronous inertia based on a UFLS limit of 59.3 Hz to prevent load shedding at a certain time after a disturbance.

	Time after disturbance (s)				
Disturbance ΔP(p.u.)		5	1	.5	.1
	.05	10.71	2.143	1.071	.2143
	.1	21.43	4.286	2.143	.4286
	.15	32.14	6.429	3.214	.6429
	.20	42.86	8.571	4.286	.8571
	.25	53.57	10.71	5.357	1.071
	.30	64.29	12.86	6.428	1.286
	.35	75.00	15.00	7.500	1.500
	.40	85.71	17.14	8.571	1.714
	.45	96.43	19.28	9.643	1.929
	.50	107.1	21.43	10.71	2.143

Equation (3.5) can be rearranged to write an expression for the time after the disturbance. This is shown in Equation (3.6) and it represents how much time there is before the frequency hits the specified maximum frequency deviation.

$$\Delta T_{max} = \frac{2\Delta\omega_{max}H}{\Delta P\omega_s} \tag{3.6}$$

Using Equation (3.6), Table 3.7 displays the time within which a frequency support mechanism would have to act in order to arrest the frequency fall before a UFLS setting of 59.3 Hz is reached, based on a known system inertia and the anticipated disturbance size. The utility of Equation (3.6) and Table 3.7 is in setting the performance benchmark, with respect to response time, that a VSG must meet in order for its response to be sufficiently timely.

In Table 3.7, a larger value is better as that means a greater margin of time for the VSG to react. The table is color coded so that 1 to 5 s is green, 500 ms to 1 s is blue, 100 ms to 500 ms is

yellow and under 100 ms is orange. The greatest available time margin comes with the largest inertia and the smallest disturbance. However, the highest value does not even reach 5 s, supporting the argument that a traditional governor response may be too slow to support a low inertia grid or a small grid whose disturbances can be more than just a few percent. Having a BESS-based VSG that can respond in under a second will allow the grid to avoid UFL where a governor response would otherwise fail. However, one second is a very conservative number for the response time of a BESS-based VSG. A more reasonable number would be between 100 and 500 ms, with some sources claiming the potential for reactions under 100 ms. That means that the yellow and blue zones could easily be covered by current technology. In other words, that is fast enough to potentially rescue the grid frequency from disturbances as high as 50% with system inertia values as low as 2 or 3. That is more that fast enough to meet the needs of most grids, even small ones.

Table 3.7: The amount of time in seconds after a disturbance before the inertial response will reach the UFLS setting of 59.3 Hz.

	The available inertia constant (s)									
Disturbance anticipated ΔP(p.u.)		2	3	4	5	6	7	8	9	10
	.05	.9333	1.400	1.867	2.333	2.800	3.267	3.733	4.200	4.667
	.10	.4667	.7000	.9333	1.167	1.400	1.633	1.867	2.100	2.333
	.15	.3111	.4667	.6222	.7778	.9333	1.089	1.244	1.400	1.556
	.20	.2333	.3500	.4667	.5833	.7000	.8167	.9333	1.050	1.167
	.25	.1867	.2800	.3733	.5667	.5600	.6533	.7467	.8400	.9333
	.30	.1556	.2333	.3111	.3889	.5667	.5444	.6222	.7000	.7778
	.35	.1333	.2000	.2667	.3333	.4000	.4667	.5333	.6000	.6667
	.40	.1167	.1750	.2333	.2917	.3500	.4083	.4667	.5250	.5833
	.45	.1037	.1556	.2074	.2593	.3111	.3630	.4148	.4667	.5185
	.50	.0933	.1400	.1867	.2333	.2800	.3267	.3733	.4200	.4667

The inertia constant that will meet the ROCOF requirement can be calculated as

$$H_{min} = \frac{\Delta P \omega_s}{2ROCOF_{max}} \tag{3.7}$$

Example results for typical anti-islanding relay settings are shown in Table 3.8. The table is color coded according to the same scheme as Table 3.6. Its entries show the minimum inertia needed to avoid triggering anti-islanding/ROCOF relays immediately after the disturbance. Compared to the minimum inertia constants in Table 3.6, the numbers in Table 3.7 are much higher if we assume a time-of-support under one second. Therefore, if we implement a BESS-base VSG then the minimum synchronous inertia should be defined by the ROCOF limits rather than the UFLS limits. Providing enough synchronous inertia to prevent triggering anti-islanding relays simultaneously prevents UFLS long enough for a BESS-based VSG to respond. It can also be observed that increasing the ROCOF settings on anti-islanding relays significantly reduces the required synchronous inertia. Doubling the ROCOF limits halves the minimum inertia.

Table 3.8: The minimum synchronous inertia to avoid triggering anti-islanding relays in the event of a disturbance.

	ROCOFmax		
Disturbance ΔP(p.u.)		0.5 Hz/s	1.0 Hz/s
	.05	3	1.5
	.10	6	3
	.15	9	4.5
	.20	12	6
	.25	15	7.5
	.30	18	9
	.35	21	10.5
	.40	24	12
	.45	27	13.5
	.50	30	15

4. BESS-based VSG for a Low Inertia System

In previous chapters we discussed how RES penetration causes problems for frequency stability, and we discussed possible solutions. In this chapter, we will simulate implementing one of these solutions, the BESS-based VSG. First, we have to consider what makes this a worthy solution compared to the other available options. Section 4.1 compares and contrasts the BESS-based VSG and the RES-based VSG to argue that the BESS is the superior option. Section 4.1 describes the strengths and weaknesses of a virtual synchronous generator relative to a traditional synchronous generator. In the course of that discussion, Section 4.1 shows how the two technologies complement each other. Section 4.2 builds on the work done in Chapter 3 to simulate a fast-acting VSG. Chapter 3 provides information for the synchronous inertia, disturbance size and time-of-response. This information is used to select the experiment parameters so that Section 4.2's simulation is not invalidated by an initial ROCOF which exceeds relay settings before the VSG can respond or by a VSG whose reaction time is too long to prevent UFLS. The purpose of Section 4.2's simulation is to determine how the size and control of the VSG affect overall frequency performance following a disturbance. Finally, Section 4.3 takes the best performing VSG from Section 4.2 and investigates how its performance varies with the delay time and rampup time constant.

4.1: The Argument for Implementing the BESS-based VSG

As seen in the literature review, there are generally two approaches to creating a VSG. One is to adapt the existing converter-coupled RES generators, and the other is to couple an energy storage system to a power converter with an appropriate control scheme. There are a number of storage technologies available for that purpose, but batteries possess an advantageous combination of cost, efficiency, response time and capacity that make them a popular choice for

VSG proposals. The two battery technologies that commonly appear in the literature and in the field are lead-acid [22] and lithium-ion [12].

Despite its name, the virtual synchronous generator differs from the real machine in key ways. Some of these differences are to the VSG's advantage and others are not. This was briefly touched on in Chapter 3, but here we shall go into more detail. It is important to understand the capabilities and limitations of both technologies. From this discussion, it shall be apparent that the VSG and synchronous generator complement each other. Both have unique roles to play in frequency stability. Both devices provide an energy buffer to address temporary power imbalances, but engineers can be much more intentional about the energy capacity of a BESS than that of a synchronous machine. Operators have much more flexibility over the charge and discharge of a BESS than over the kinetic energy reserves of a synchronous machine. The timing and control law of a BESS's power flow can easily be adjusted, whereas that of a synchronous machine is largely fixed by its inertia [26]. The operators of a synchronous plant have no control over its inertial response. The BESS's flexible control allows it to adapt to changing grid conditions. Rapid grid changes are becoming more of a reality as more renewables are integrated.

However, the synchronous generator cannot be done away with, for it fulfills a number of roles that would be impractical for a VSG to emulate. First, the synchronous machine provides its initial response without delay. As demonstrated in the previous chapter, the inertial response of the synchronous generator enables the synthetic inertia response by buying enough time for a BESS to act. The VSG then returns the favor by taking some of the burden off the synchronous generators. In this way, the synchronous and virtual inertial responses complement each other. A BESS VSG can provide inertia emulation, primary frequency control and even secondary

frequency control (if it has enough capacity to last that long), but it is impractical for tertiary frequency control [42]. Tertiary frequency control provides power point adjustments for indefinite steady-state. A BESS cannot operate with an indefinite power flow. The longer a BESS has to provide power, the larger it has to be, which means the more expensive it will be. A synchronous generator is well-suited to providing power for an indefinite period of time. The controllability of a BESS makes it good for quickly stabilizing the system, but the endurance of a synchronous generator makes it ideally suited for making long-term steady-state adjustments. A VSG can deliver a primary frequency control much faster than a synchronous machine [12]. Whereas the synchronous generator has to wait seconds for its governor-turbine apparatus to adjust, a BESS-based VSG's frequency response can be delivered simultaneously with its inertia emulation. Delivering a faster primary frequency control is important because that is what brings the frequency to steady-state. The sooner that steady-state can be achieved, the less need there is for the inertial response. Another potential benefit of using BESS-based VSGs to provide primary frequency control is that there becomes less of a need to deload generators since BESS can provide the necessary headroom for frequency response. This increases the utilization of the remaining generators, so fewer generators are needed, reducing overall generation costs.

Although there is a considerable body of literature devoted to describing RES-based VSGs, there are a number of reasons why this is not an ideal solution. Consider how a typical RES generator is operated. Usually, wind and solar plants output the maximum power they can, and their converters do not implement inertia response or frequency response controls. There are good reasons to operate wind and solar plants in this way. The owner of the plant is not responsible for system stability. That is the operator's job. The plant owner just wants to maximize its profits. Operating a RES plant in a way that supports frequency stability

traditionally runs counter to the profit motive. The additional controls needed to implement inertia emulation or frequency response on a converter would add to its cost. Even if such controls were added, they require that the generators have some headroom to increase their power output. Wind and solar plants have strong incentives to operate at their maximum power point. This is because, unlike conventional power plants, wind and solar generators incur little to no additional operating costs for increasing their power point. To deload a wind or solar plant would be leaving free money on the table. But without deloading, the plants have no headroom to provide frequency response. It is an economic issue, not a technical one, that is arguably the biggest impediment to RES-based VSG. The technology is there to make it happen, the question is who will pay for it. The added expense and the lost profit potential will be hard to justify to RES plant owners unless they are compelled by regulations or incentivized by market structures. This is why the discussion on RES integration frequently involves updating grid codes and ancillary service markets [4],[3],[28]. Either way, implementing VSGs on wind and solar plants will increase their costs and decrease the capacity factor.

Even if the economic factors were ignored, there are technical reasons why a grid with BESS-based VSGs may be superior to a grid with RES-based VSGs. Wind and solar plants are notorious for intermittency. That intermittency can degrade the effectiveness of wind and solar-based VSGs. To illustrate why this is the case, consider the following example: A power system has significant levels of wind penetration and the operators have decided to compensate by turning many of those wind plants into VSGs. If the wind suddenly dies out, that will create a disturbance via a loss of generation. Since there is not enough synchronous generation to correct a disturbance alone, the system is relying on the wind plants to help out. However, as was illustrated by [10], the strength of the virtual inertia depends on the wind speed. Worse, a sudden

drop in wind may wipe out any generator headroom, making primary frequency control from the VSG defunct. So right when the VSG's response is most needed, its capabilities are attenuated. The fall in wind speed not only causes the disturbance but also defeats the countermeasure. This is not to say that VSGs from wind plants are useless, but that they are not a robust solution. They are a satisfactory solution for addressing sudden shifts in load, but not for generation. Using solar plants for VSGs is even worse. Like wind, solar plants can be deloaded to provide headroom for frequency response [3]. But solar's headroom runs into the same intermittency issues as wind. At night, no solar headroom is possible, and it is well known that the grid tends to be more sensitive to disturbances at night due to its low-load condition. As with the wind example, the solar response may not be available when it is needed. Unlike wind, solar does not have a significant energy buffer to draw from, so an ESS would have to be attached to achieve parity, further adding to its already high capital costs. In that case, why not simply have the ESS stand on its own? It does not need to be attached to a PV unit to serve as a VSG. A BESS-based VSG does not care whether it is day or night, windy or calm. A BESS is consistent. Furthermore, a BESS-based VSG would not suffer the economic tradeoffs of a RES-based VSG. Instead of making money by selling energy, a BESS could be profitable by selling frequency services [22]. This would free up wind and solar plants to focus on what they do best: producing as much clean energy as possible.

4.2: Sizing and Control of a BESS-based VSG

This chapter builds upon the simulation model used in Chapter 3 by adding a VSG to the bus. This section studies the different ways that a VSG can be controlled and sized and then compares their effects on the frequency and ROCOF following a reasonable disturbance. One

control method is inertia emulation/inertia control. It mimics the behavior of the swing equation through a derivative control law.

$$P_{vsg} = k_d \frac{d\omega}{dt} \tag{4.1}$$

Inertia control provides ROCOF services, slowing the rate of frequency decline after the disturbance. The next control method is primary frequency control, which is also sometimes called frequency response. The term "fast frequency response" is sometimes used to refer to a primary frequency control that can be delivered faster than is typical, such as that which can be provided by a BESS. This control method mimics the governor-turbine droop control of synchronous generation.

$$P_{vsg} = k_p(\omega - \omega_s) \tag{4.2}$$

In a VSG, both methods are implemented as an electronic control system. The nature of such control systems allows us to seamlessly blend the two into one combined control of inertia control and primary frequency control.

$$P_{vsg} = k_d \frac{d\omega}{dt} + k_p(\omega - \omega_s) \tag{4.3}$$

To make the BESS behavior more realistic in simulation, a reaction time is implemented. The reaction time is split into a delay time and a ramp time. The delay is the amount of time after the disturbance that it takes for the BESS to begin providing power. This reflects the time it takes for the BESS to detect a disturbance and issue the command to act. The ramp time is modeled differently than the rampup described by [12]. That study considered a linear ramp rate based on a BESS that was mainly providing frequency response. The rampup in [12] was linear because it was proportional to the linear fall in frequency. Since inertia emulation is a major consideration in this chapter, a linear ramp is not appropriate for this study. Instead, this study uses a ramp that is modeled by a time constant delay function. This is meant to reflect the fact that a battery can

typically be modeled as a voltage source connected to a RC circuit [43] and RC circuits are nonlinear by nature. Thus, the control law governing the BESS's reaction time is expressed by the following:

$$P_{vsg} = \begin{cases} 0 & for\ T < T_o + T_{delay} \\ \left(1 - e^{-\frac{\Delta t}{T_{ramp}}}\right)(Control\ Output) & for\ T \geq T_o + T_{delay} \end{cases} \quad (4.4)$$

Here, P_{vsg} is the output power of the VSG. The time is T. The time of the disturbance is T_o. The delay time is T_{delay}. The amount of time that is passed since the VSG begins ramping up is Δt. The BESS time constant is T_{ramp}. Finally, *Control Output* is what comes out of Equations (4.1), (4.2), and (4.3).

The scenario used in this section has a synchronous generator with a relatively low inertia of H = 3. Given the inertia we have to work with, we can then turn to Table 3.8 to see how large a disturbance the system can handle without triggering ROCOF relays. In this study, it is assumed that the relays will trip if the ROCOF exceeds 1 Hz/s. Therefore, the system with H = 3 can handle a 10% disturbance or less, and so that is the disturbance size used in this study. Operators will need to ensure that there is sufficient synchronous inertia connected in the system to prevent ROCOF relays from immediately tripping after a disturbance. If that is impossible, then their other options include increasing relay settings and taking measures to reduce the chances of a large disturbance. Now that we know the given inertia and the anticipated disturbance size, we can turn to Table 3.7 to determine how fast the VSG must react in response to the disturbance in order to avoid UFLS. According to Table 3.7, the VSG must respond within 700 ms of the disturbance to prevent the frequency from falling to 59.3 Hz. That is more than enough time given the available technology. A delay time of 150 ms and a time constant of 150 ms were chosen for this model as these are reasonably attainable numbers for a BESS [12].

This study looks at the impact of VSG sizing on performance. To clarify, within the context of this study, "size" refers to the rated power of the VSG and not its energy capacity. The size of the VSG determines the control gain parameters according to the heuristic described by [15],[21]. The inertia control constant k_d is chosen so that the VSG outputs its maximum power at the maximum allowable ROCOF.

$$k_d = \frac{P_{vsg\_nominal}}{ROCOF_{max}} \tag{4.5}$$

Similarly, the primary frequency control constant k_p is chosen so that the VSG outputs its maximum power at the maximum allowable frequency deviation.

$$k_p = \frac{P_{vsg\_nominal}}{\Delta\omega_{max}} \tag{4.6}$$

The gain k_d should be set negative so that inertia control opposes any deviation in ROCOF from zero. The gain k_p should be set negative so that primary frequency control opposes any deviation in frequency from nominal. In this way, as the frequency falls both inertia control and primary frequency control will direct the VSG to supply power to the grid.

Figures 4.1, 4.2, and 4.3 show the frequency of the system, the output power of the VSG, and the ROCOF of the system, respectively, for an undermatched VSG. Within the context of this study, "undermatched" means that the size of the VSG is less than the size of the disturbance. In this case, the VSG is sized to be 80% of the disturbance. The three control cases are overlaid on the same charts for comparison, along with the base case to provide a reference. It can be observed from Figure 4.3 that the ROCOF is -1 Hz/s immediately after the disturbance. The VSG starts to send power 150 ms later, as seen in Figure 4.2, which reduces the generation-load imbalance. This causes the ROCOF to move closer to zero in all three VSG control cases. It can be observed from Figure 4.3 that the ROCOF reaches a steady-state non-zero value for all cases. An undermatched VSG cannot supply enough power to fully cover the generation-load

imbalance. The remainder must continue to be supplied by the stored kinetic energy of synchronous generation. Figure 4.3 also shows that the ROCOF is most attenuated with either primary frequency control or primary frequency control plus inertia control, both of which reduce the magnitude of the ROCOF by over 80%. In contrast, the use of inertia control only attenuates the ROCOF by a little under 50%. From this comparison, it is clear that pure inertia control does not produce the best possible effects on ROCOF.

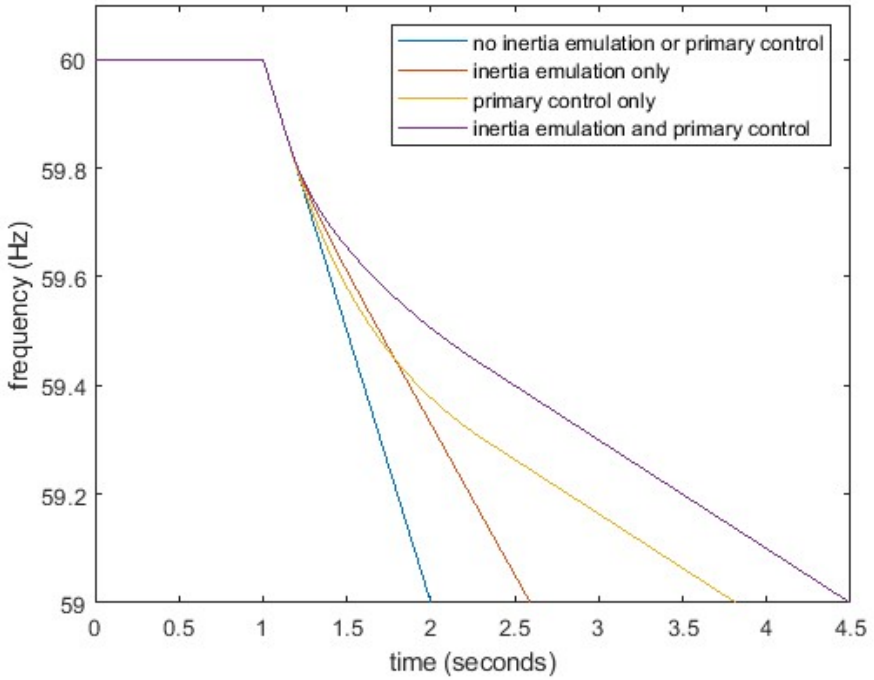

Figure 4.1: Frequency of the system with VSGs that are sized to be 80% of the disturbance size (undermatched). H = 3 and the disturbance size is 0.1 p.u.

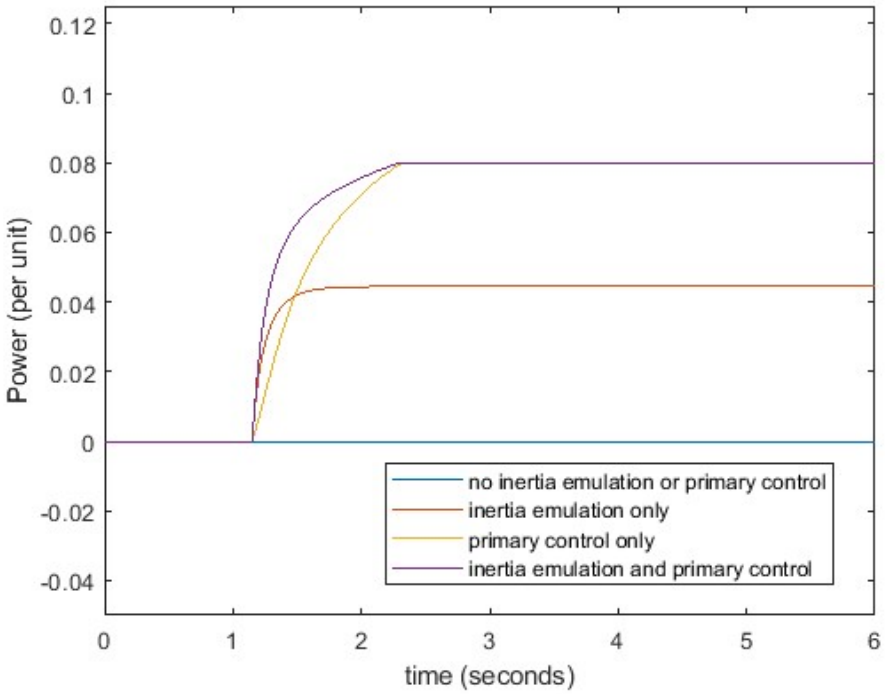

Figure 4.2: Power output from VSGs that are sized to be 80% of the disturbance size (undermatched). H = 3 and the disturbance size is 0.1 p.u.

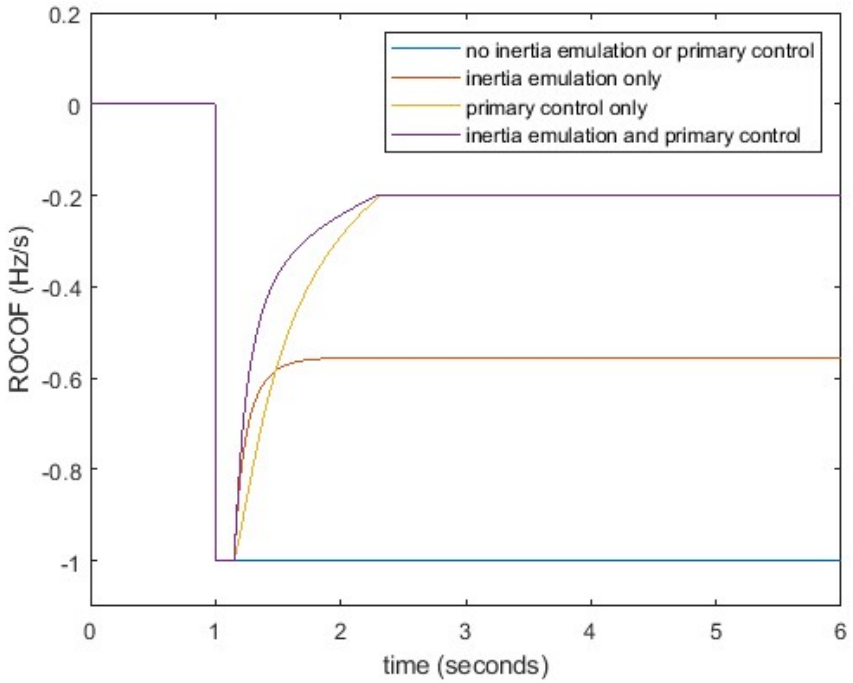

Figure 4.3: ROCOF of the system with VSGs that are sized to be 80% of the disturbance size (undermatched). H = 3 and the disturbance size is 0.1 p.u.

Although primary frequency control does do better in the long run, it suffers from a relatively long rampup to full power. This slow ramp rate is the consequence not of the battery time constant, which is fairly short, but of proportional control. The frequency deviation starts off small, which means the primary frequency control also starts off small, and then they both grow over time. In contrast, the output of the inertia emulation quickly ramps up to its steady-state value because the ROCOF starts off large. Because of this quick start, inertia control initially has a better impact on the ROCOF than primary frequency control, but the power output from inertia control quickly settles while the power from primary frequency control continues to grow and eventually overtakes inertia control. The reason why the power output from primary frequency control does not continue to grow after a certain point is that the VSG reaches its maximum power limit.

We can get the best of both worlds by combining inertia control and primary frequency control. Shown in purple in the figures, the combined control has the fast rampup of inertia control and the high steady-state power output of primary frequency control. The result is an overall superior ROCOF performance. In particular, the combined control produces a better short-term ROCOF performance than primary frequency control used alone. Even though they both settle at the same steady-state ROCOF, the early lead from the combined control manifests itself in Figure 4.1 as a significant advantage in frequency over primary frequency control. Thus, the combined control would yield more time until the frequency nadir. Inertia control also has an early lead over primary frequency control, but that does not translate into a long-term advantage in frequency because inertia control does not reach the same steady-state power output as the other two cases.

The steady-state ROCOF from inertia control can be calculated. To derive the approximate formula, start with Equations (4.7), (4.8), and (4.9).

$$\frac{2H}{\omega_s} ROCOF = P_m - P_e \tag{4.7}$$

$$P_e = P_{load} - P_{vsg} \tag{4.8}$$

$$P_{vsg} = K_d ROCOF \tag{4.9}$$

Combine these equations through substitution, then rearrange terms to get an expression for the ROCOF. This yields Equation (4.10).

$$ROCOF = \frac{\omega_s (P_m - P_{load})}{2H - k_d \omega_s} \tag{4.10}$$

In our example of an undermatched VSG, $\omega_s = 2\pi 60$, $P_m = 1$, $P_{load} = 1.1$, H = 3 and $k_d = -0.0127$. The ROCOF calculated by Equation (4.10) is -3.495 r/s^2 or .556 Hz/s, which matches what we see in Figure 4.3.

In the case of the combined control and primary frequency control of an undermatched VSG, the steady-state ROCOF comes about when the VSG reaches its power limits. Based on this observation, we can derive a formula for the steady-state ROCOF of an undersized VSG with primary frequency control or combined control. To do this, take Equation (4.11) and substitute it into Equation (4.7). Rearrange the terms to isolate ROCOF. This produces Equation (4.12).

$$P_e = P_{load} - P_{vsg\_nominal} \tag{4.11}$$

$$ROCOF = \frac{\omega_s}{2H} (P_m - P_{load} + P_{vsg\_nominal}) \tag{4.12}$$

With $P_{vsg\_nominal} = 0.08$ (80% of the disturbance size), the ROCOF calculated by Equation (4.12) is -1.2567 r/s^2 or -0.2 Hz/s which matches what we see in Figure 4.3

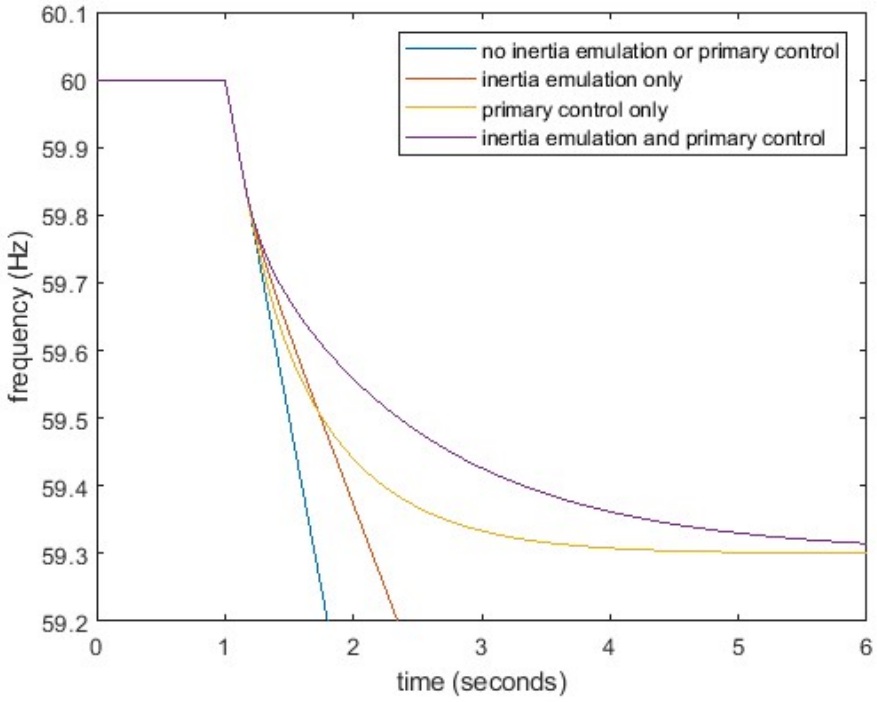

Figure 4.4: Frequency of the system with VSGs that are sized to be the same as the disturbance size (matched). H = 3 and the disturbance size is 0.1 p.u.

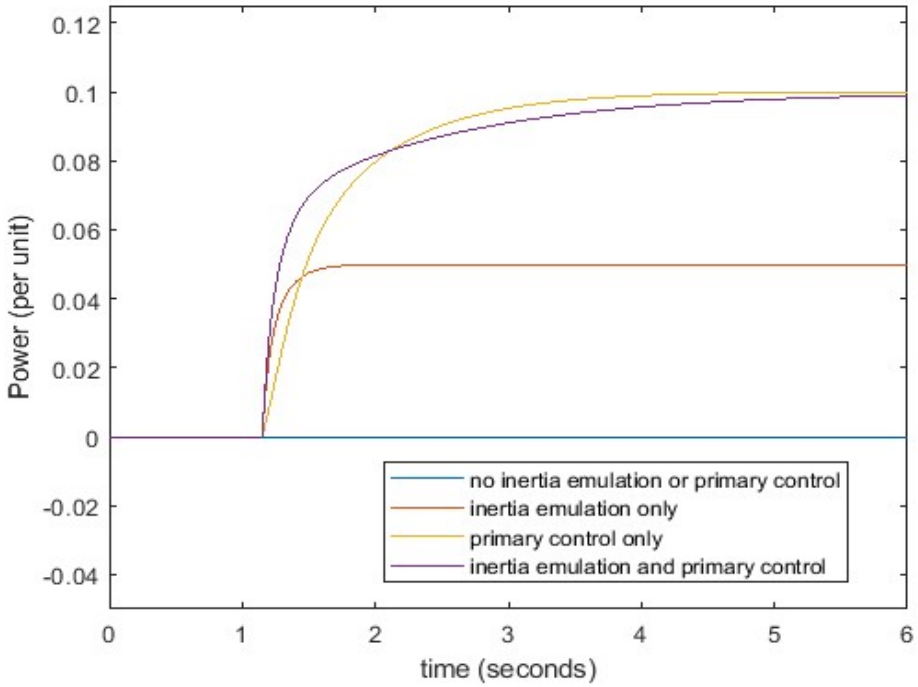

Figure 4.5: Power output from VSGs that are sized to be the same as the disturbance size (matched). H = 3 and the disturbance size is 0.1 p.u.

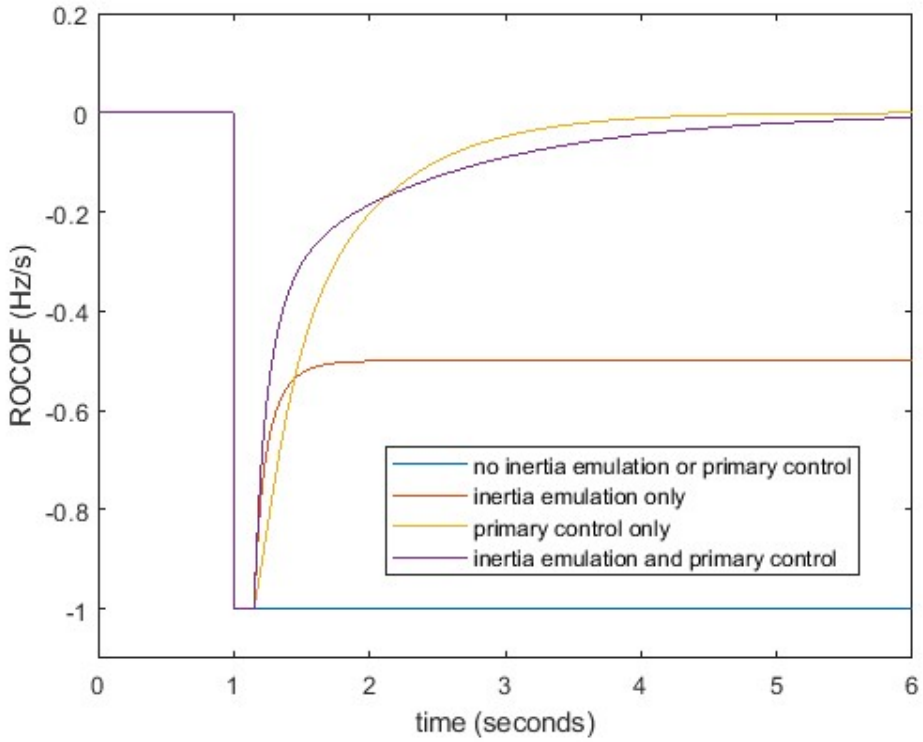

Figure 4.6: ROCOF of the system with VSGs that are sized to be the same as the disturbance size (matched). H = 3 and the disturbance size is 0.1 p.u.

Next, we consider the case of a "matched" VSG where the VSG's nominal power equals the size of the disturbance. The results are shown in Figures 4.4, 4.5, and 4.6. We can observe differences between these results and that of the undermatched case that was just discussed. When the VSG could not completely cover the generation-load imbalance, the remainder had to come from slowing down the synchronous generation. For the VSG to bring the frequency to steady-state under its own power, it must be able to supply power equal to the size of the disturbance so that there is no more imbalance to make up for. This is the case of the matched VSG. Figure 4.4 shows that both primary frequency control and combine control bring the frequency to steady state. Figure 4.6 reflects this by showing the ROCOF converging to zero for those controls. Figure 4.5 shows something that Figure 4.2 does not: the power output of primary frequency control briefly overtakes that of the combined control. The effects of this phenomenon

manifest in Figure 4.4. Initially, the combined control's early lead in power gives it a frequency advantage over primary frequency control. However, thanks to primary frequency control's power boost, that gap narrows over time and the frequency from primary frequency control is almost able to catch up to the combine control. The combined control still retains a slight lead in frequency by the end of the simulation, so its overall performance can still be considered superior. As with an undermatched VSG, the inertia control has the worst performance of the three. Even with a VSG that is capable of closing the power imbalance, inertia control does not order enough power to drive the ROCOF to zero. This is because inertia control is a form of derivative control and derivative action is incapable of bringing a system to steady-state on its own. Inertia control from a matched VSG does at least perform better than from an undermatched VSG due to the higher gain constant produced by Equation (4.5).

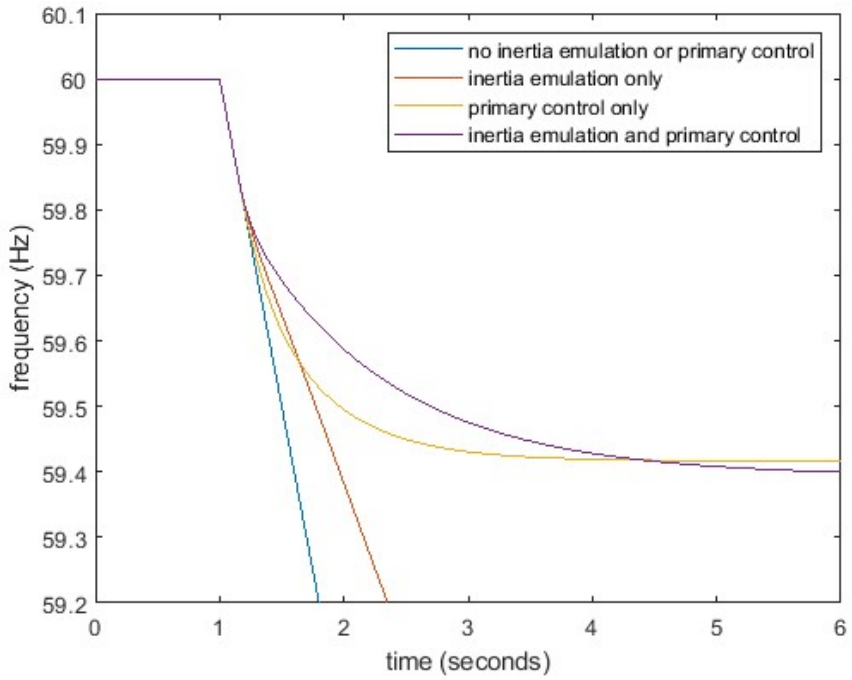

Figure 4.7: Frequency of the system with VSGs that are sized to be 20% greater than the disturbance size (overmatched). H = 3 and the disturbance size is 0.1 p.u.

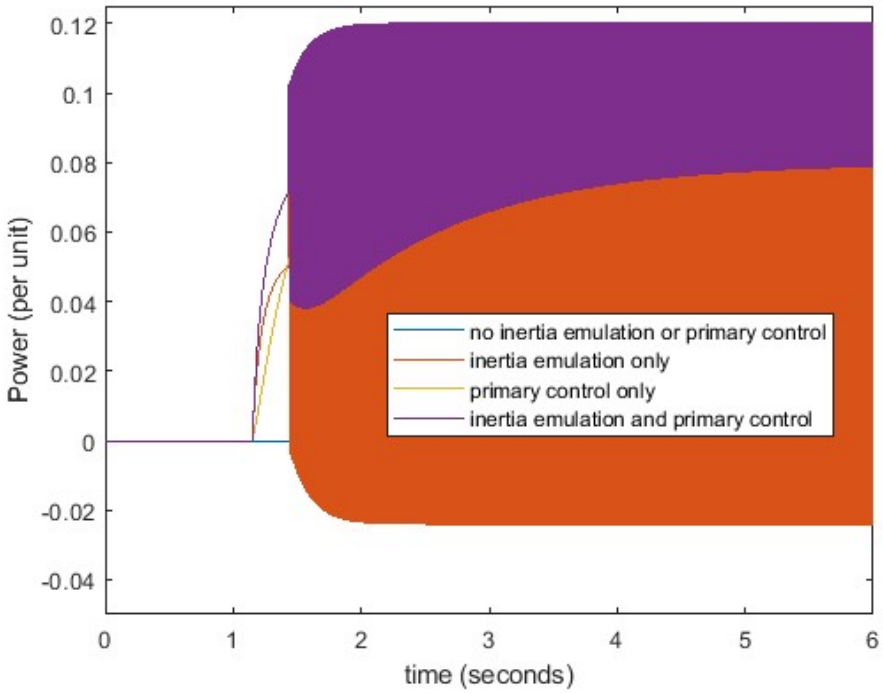

Figure 4.8: Power output from VSGs that are sized to be 20% greater than the disturbance size (overmatched). H = 3 and the disturbance size is 0.1 p.u.

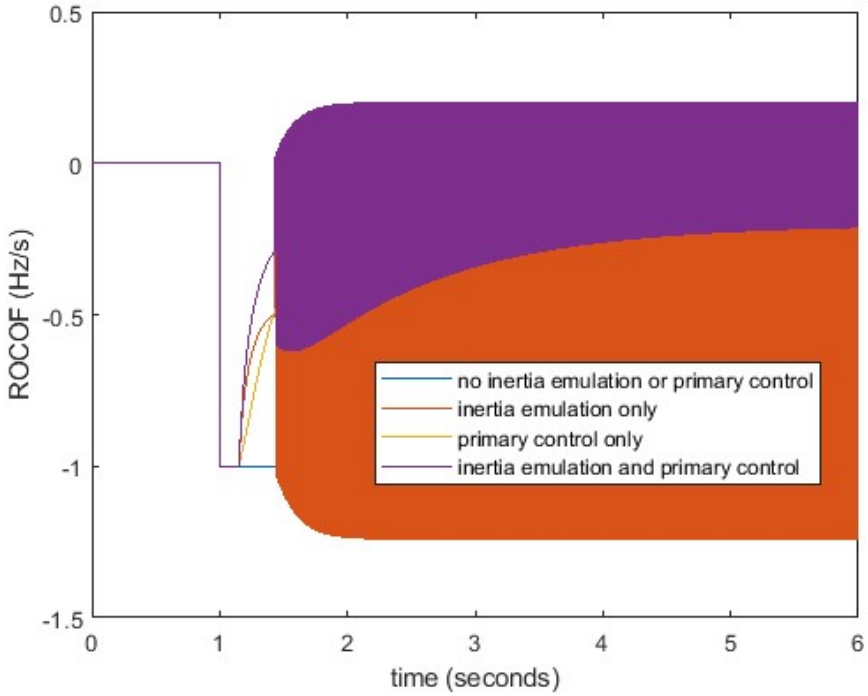

Figure 4.9: ROCOF of the system with VSGs that are sized to be 20% greater than the disturbance size (overmatched). H = 3 and the disturbance size is 0.1 p.u.

Although a matched VSG can bring the frequency to steady-state, Figure 4.4 shows that it just barely avoids UFLS at 59.3 Hz. A more powerful VSG might be better so as to have a comfortable safety margin. However, a problem arises when the nominal power of the VSG is increased to the point where it "overmatches" the size of the disturbance. The results of a 20% overmatch are shown in Figures 4.7, 4.8, and 4.9. From Figure 4.7 alone, it may seem like bigger is indeed better. The frequencies of both primary frequency control and combined control settle higher here than for the matched VSG. But that is not the full story. Figure 4.8 shows that combined control, along with inertia control, is seized by a very high frequency power oscillation. These oscillations have a particularly deleterious effect on the inertia control. The oscillations in inertia control's power cross into the negative region, which causes the ROCOF to go past -1, as shown in Figure 4.9. In general, power oscillations such as these are not good for the health of the equipment. Notice that both combined control and inertia control have the inertia control in common. That is the culprit. The inertia control constant k_d was sized so that the VSG would output its maximum power at the maximum ROCOF. While this heuristic is intuitive, there can be an issue when the VSG overmatches the disturbance because the inertia control can overshoot and inject much more power into the system than is needed. That causes the ROCOF to go from a large negative value to a large positive value, which is no improvement. The inertia control reacts to this "mistake" by repeating the mistake in the opposite direction, and the cycle continues. The problem is that Equation (4.5) produces a control gain that is inappropriately large for an overmatched VSG. Recall that the inertia control was stable for the matched case. Therefore, instead of sizing k_d according to the VSG's nominal power, let us size it according to the size of the disturbance.

$$k_d = \frac{disturbance\ size}{ROCOF_{max}} \tag{4.13}$$

Using Equation (4.13) to generate k_d of an oversized VSG produces stable power output. The proof of this is visible in Figures 4.10, 4.11, and 4.12. The shapes of the curves are similar to those of the matched VSG. The adjusted overmatched VSG has the same k_d as the matched VSG but has a higher k_p than the matched VSG. Comparing Figure 4.10 to Figure 4.4 shows that after the oscillations are eliminated an overmatched VSG does produce a better settling frequency for primary frequency control and combined control. This illustrates the benefit of a more powerful primary frequency control. Figure 4.11 shows that the overmatched VSGs do not reach their nominal power limit of 1.2. This suggests that there is still room for a more powerful primary frequency control. So not only does Equation (4.5) oversize the inertia control for an overmatched VSG, but Equation (4.6) undersizes its primary frequency control. As a demonstration, k_p was doubled and resulted in Figures 4.13, 4.14, and 4.15. Doubling k_p significantly reduced the time it took to bring the ROCOF to zero, which resulted in higher settling frequencies.

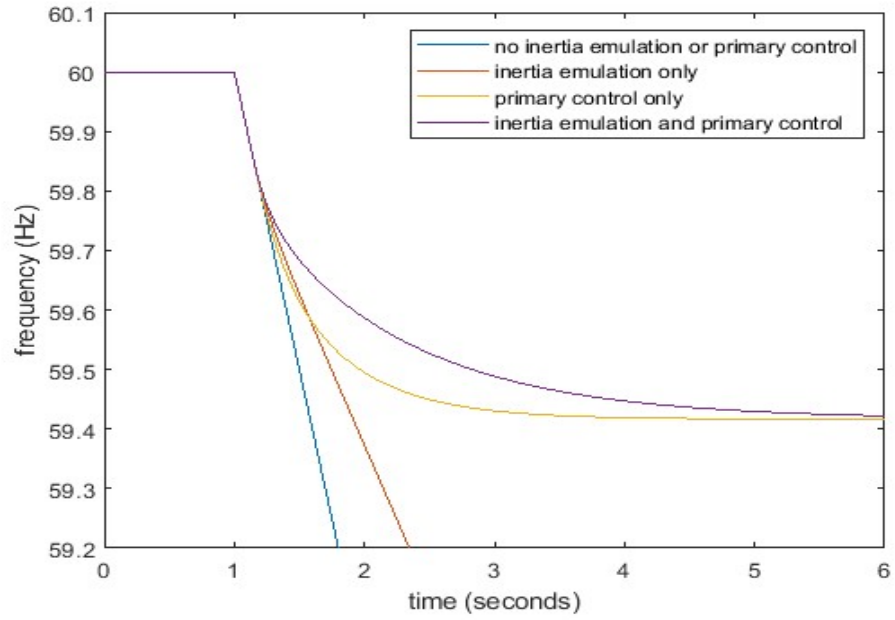

Figure 4.10: Frequency of the system with VSGs that are sized to be 20% greater than the disturbance size. The gain constant k_d is calculated with Equation (4.13).

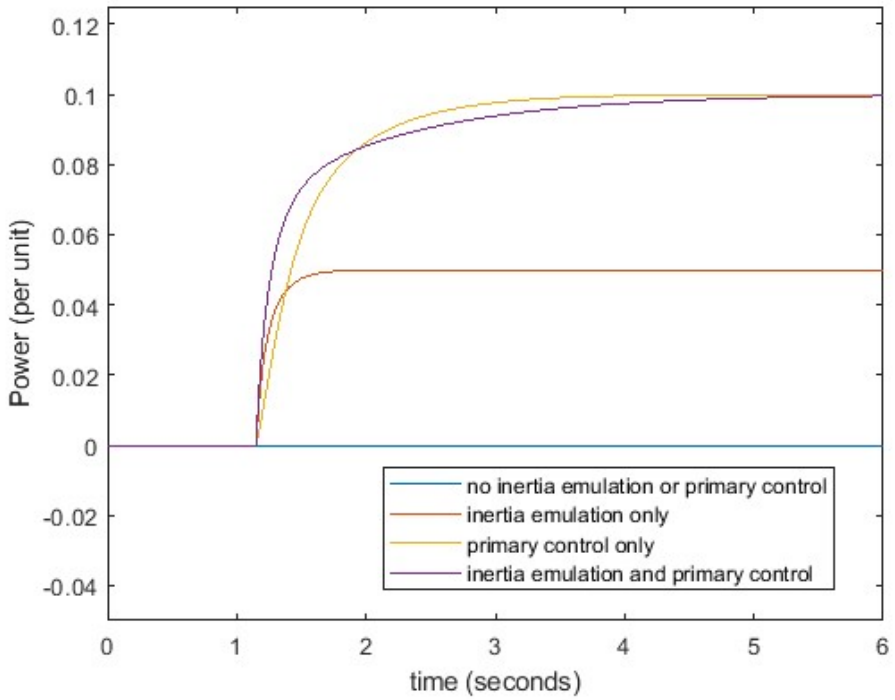

Figure 4.11: Power output from VSGs that are sized to be 20% greater than the disturbance size. The gain constant k_d is calculated with Equation (4.13).

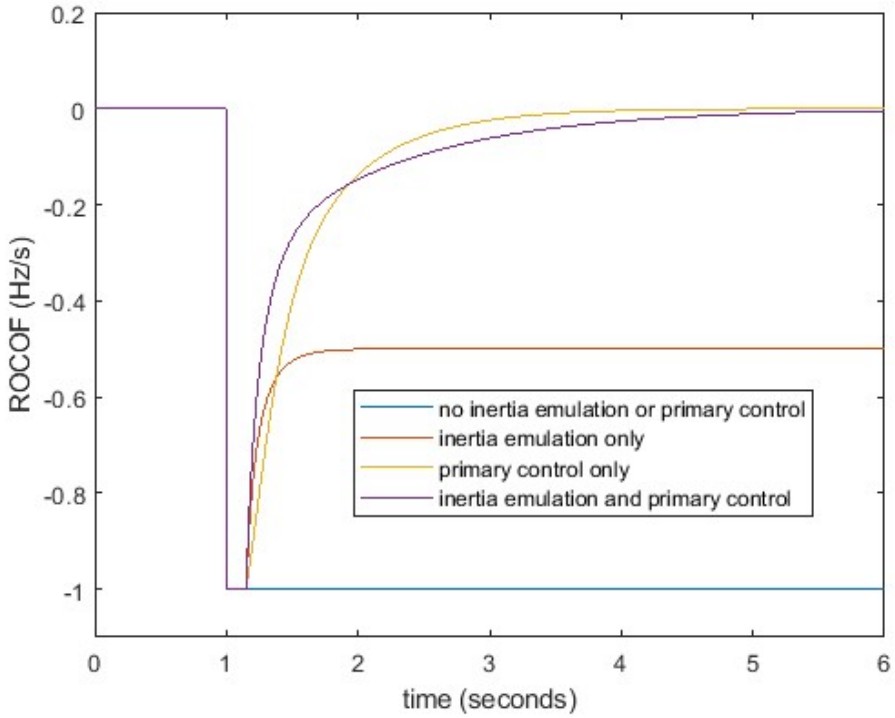

Figure 4.12: ROCOF of the system with VSGs that are sized to be 20% greater than the disturbance size. The gain constant k_d is calculated with Equation (4.13).

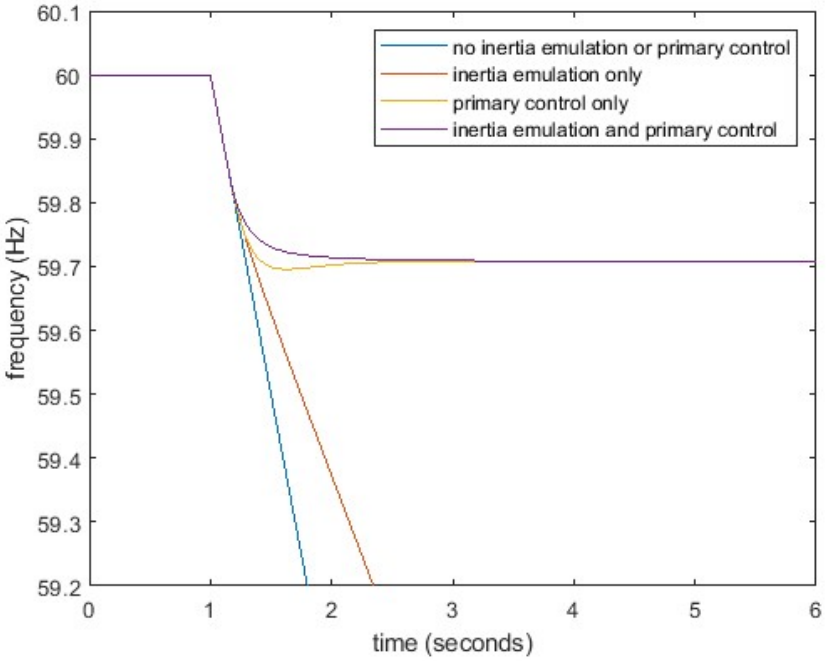

Figure 4.13: Frequency of the system with VSGs that are sized to be 20% greater than the disturbance size. The gain constant k_d is calculated with Equation (4.13). The gain constant k_p is doubled.

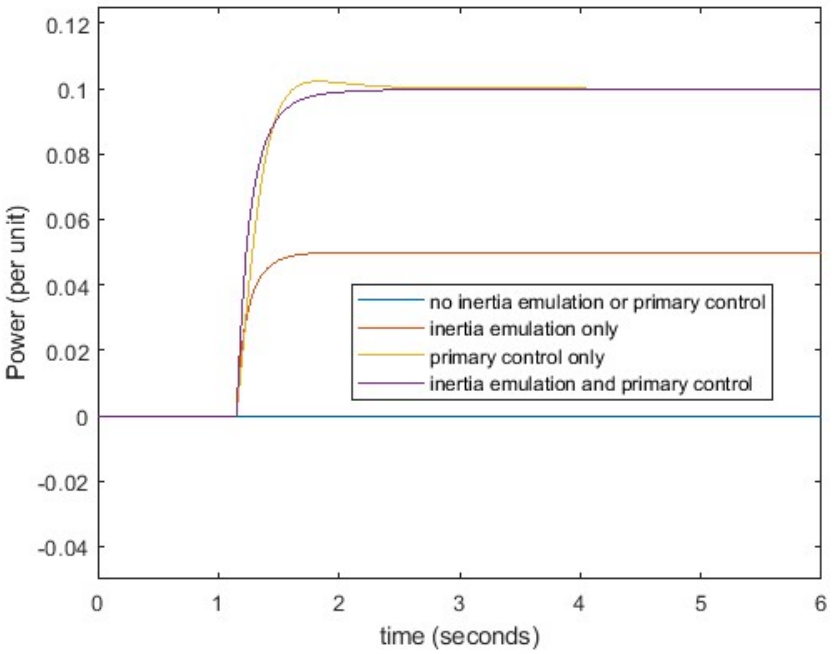

Figure 4.14: Power output from VSGs that are sized to be 20% greater than the disturbance size. The gain constant k_d is calculated with Equation (4.13). The gain constant k_p is doubled.

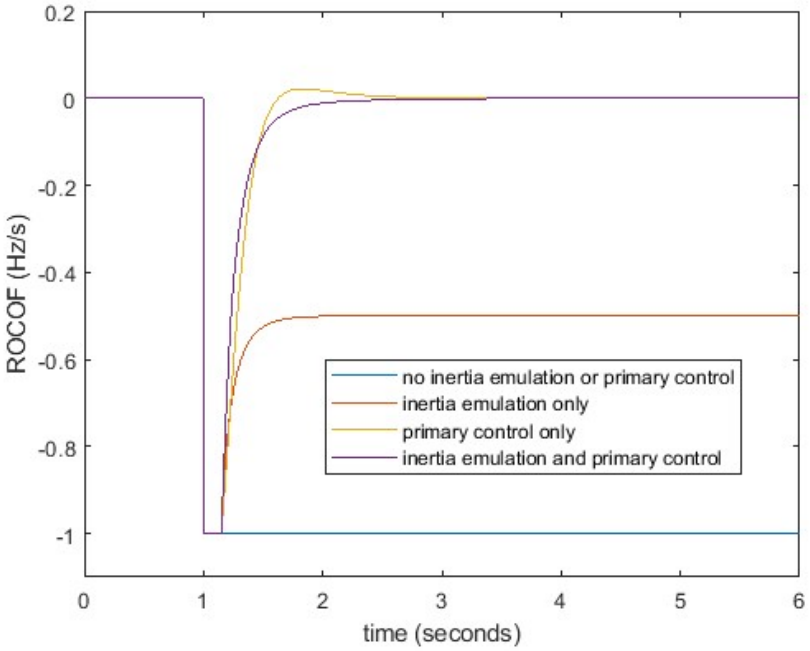

Figure 4.15: ROCOF of the system with VSGs that are sized to be 20% greater than the disturbance size. The gain constant k_d is calculated with Equation (4.13). The gain constant k_p is doubled.

We can conclude from these results that combined control delivers the best overall performance. The next best option is primary frequency control, and then inertia control is better than nothing. In general, a bigger VSG performs better. When undermatched, having a more powerful VSG will slow the rate of frequency decline. Once the size of the VSG meets or exceeds the size of the disturbance, it is strong enough to bring the frequency to steady-state under its own power. An undermatched VSG is still useful to the system because it reduces the chances of tripping ROCOF relays and delays the frequency nadir, which buys time for slower frequency response mechanisms to kick in. The heuristics provided by Equations (4.5) and (4.6) are adequate for controlling an undermatched or matched VSG, but an overmatched VSG cannot be controlled in the same way. The inertia control constant should be set according to the size of the disturbance, or lower, in order to avoid potentially damaging oscillations. The primary frequency control gain can be much higher than what Equation (4.6) indicates, and a more

powerful primary frequency control is linked to better performance, especially when supported by a moderate inertia control.

4.3: Timing of an Overmatched VSG with Combined Control

Section 4.2 used a fixed delay time and time constant of 150 ms to evaluate a number of different VSG control and sizing schemes for a given system and disturbance. This section uses the same system inertia and disturbance as Section 4.2 and uses the best VSG configuration that was tested. That means using a combined control comprising inertia control and primary frequency control. The VSG is oversized by 20% over the disturbance. Its control gains are determined by Equations (4.13) and (4.14).

$$k_p = \frac{2P_{vsg\_nominal}}{\Delta\omega_{max}} \tag{4.14}$$

The purpose of this section is to take the best VSG from Section 4.2 and look at how the delay time and ramp time constant affects its performance. First, the time constant is fixed at 0.15 and the delay time is varied. The resulting overlaid frequency and power waveforms are on display in Figures 4.16 and 4.17 respectively. Figure 4.16 shows that the frequency is brought to steady-state regardless of the delay time and that the delay time has a negligible effect on the value of the steady-state frequency. However, the delay time does have a significant impact on the nadir frequency. For delay times under about 0.2, the frequency gradually falls to its steady-state value, never dipping below it. This is reflected in Figure 4.17 where the corresponding power curves gradually match, but never exceed, the size of the disturbance. From a stability perspective, such a short delay would be ideal as it eliminates the risk of UFLS as long as the control gains are high enough that the steady-state frequency is above the UFLS setting. For delays greater than 0.2, a dip develops in the frequency curve that falls lower and lower as the delay time increases. If the delay time goes past 0.6 then the VSG will be unable to prevent

UFLS at 59.3 Hz despite the fact that Table 3.7 says the time-of-response should be 0.7 or less. The reason for this is that the frequency will not start to climb until the VSG power matches the disturbance, but that does not happen right after the delay. Figures 4.16 and 4.17 show that the nadir frequency does not occur at the time the VSG begins ramping power. Rather, the nadir frequency is reached later once the power climbs to 0.1 (the size of the disturbance). Therefore, the delay time must be smaller than the time-of-response listed in Table 3.7. A more precise interpretation is to say that the VSG must match the disturbance before the time listed in Table 3.7 unless the reaction is fast enough such that there is no nadir below the steady-state frequency. Besides improving the delay time, improving the ramp time can help shift the nadir frequency up, as demonstrated by Figure 4.18 in which the ramp time constant was decreased from 0.15 to 0.05.

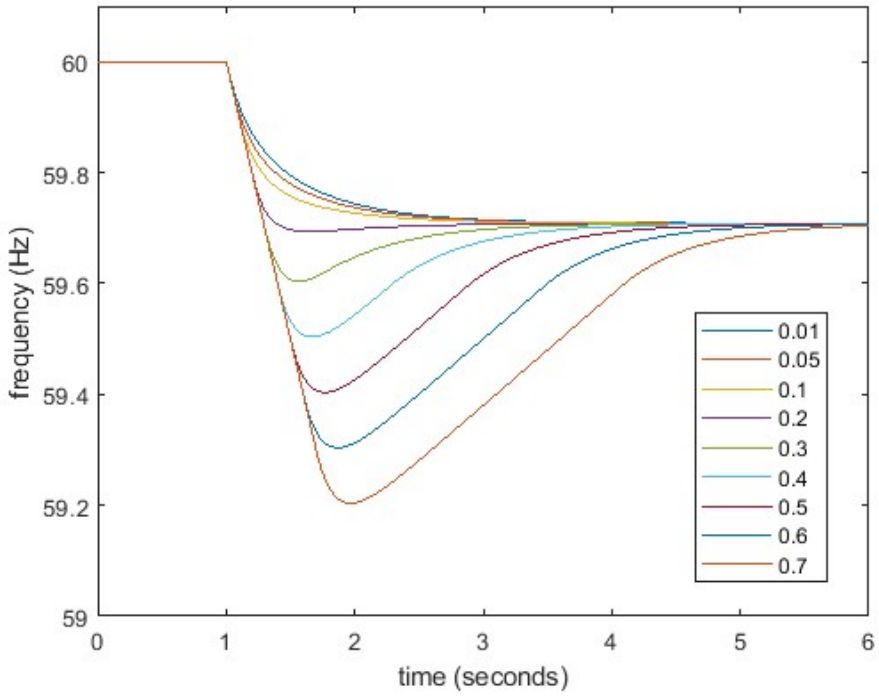

Figure 4.16: Overlaid system frequencies of a 20% overmatched VSG with combined control for different delay times. Time constant = 0.15.

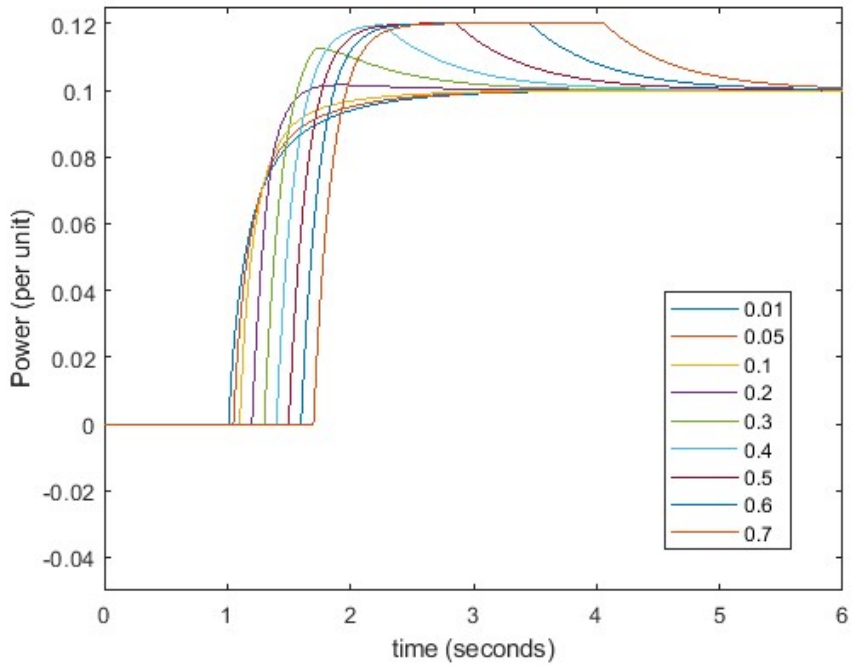

Figure 4.17: Overlaid VSG power outputs of a 20% overmatched VSG with combined control for different delay times. Time constant = 0.15.

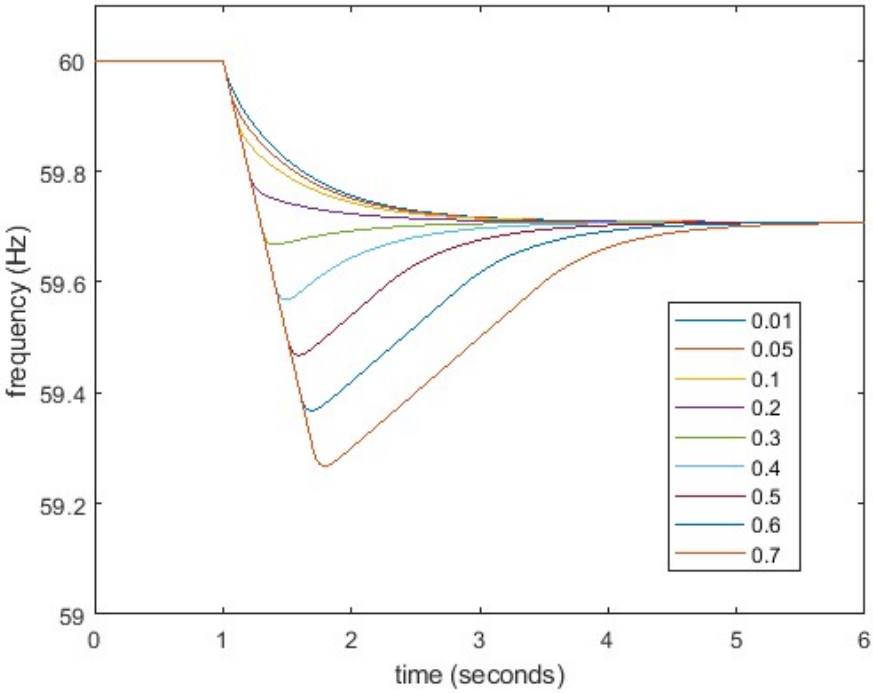

Figure 4.18: Overlaid system frequencies of a 20% overmatched VSG with combined control for different delay times. Time constant = 0.05.

Figure 4.17 shows how the VSG power curve is more gradual when the delay time is low. When the delay is short, the VSG begins powering up while the frequency deviation is small. As a result, its primary frequency control starts off weak and the response is dominated by the inertia control. As already seen in Figures 4.5, 4.11 and 4.15, inertia control does not exhibit overshooting behavior and that is reflected in the low delay power curves. However, primary frequency control still has an important influence on those power curves. As the frequency approaches its steady-state value, the ROCOF approaches zero which causes the inertia control to die out. Meanwhile, the frequency deviation gets larger, which empowers the primary frequency control. So, for a short delay the inertia control dominates in the beginning and the primary frequency control takes over in the end.

When the delay is longer the power curve becomes steeper, meaning the VSG is responding more aggressively. A longer delay allows the frequency deviation to grow more. When the VSG begins to react, it does so with a much stronger primary frequency control than if it had reacted earlier. The VSG's initial power command grows stronger as the delay time increases, but only up to a point. Eventually, the initial power command runs into the maximum power limits. That means when the delay is long enough the VSG tries to make up for lost time by putting out as much power as it can, as fast as it can. In Figure 4.17, the rampups for the 0.7, 0.6, 0.5 and 0.4 second curves look the same because the time constant determines the rampup profile. At lower delays, the evolution of the primary frequency control plays a role in shaping the curve, but there is no room for that to happen with a high delay because the combination of high ROCOF and large frequency deviation compels the VSG to ramp up as fast as it can. This means that a long delay time puts pressure on the VSG to have a short time constant, while a short delay time allows longer time constants. Decreasing the delay, which can mainly be

achieved through faster disturbance detection, could allow other, slower ramping storage technologies to serve a VSG.

With a high delay, the VSG power remains maxed out for some time before coming down to a steady-state value. When the VSG is putting out more power than the size of the disturbance, it is injecting energy into the system to speed up the frequency. Eventually, the power comes down to match the disturbance so as to stabilize the frequency. The longer the delay, the more energy the VSG has to inject into the system to achieve the same end. This is bad because it would require a larger energy capacity, increasing the expense of the storage system. Reacting early means less energy, and therefore less capacity, is needed.

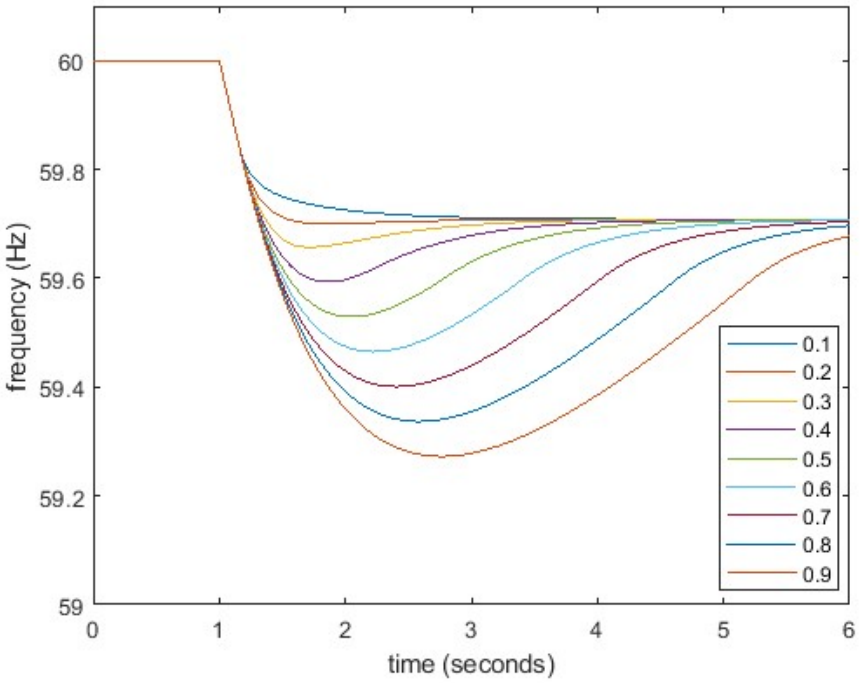

Figure 4.19: Overlaid system frequencies of a 20% overmatched VSG with combined control for different time constants. Delay time = 0.15.

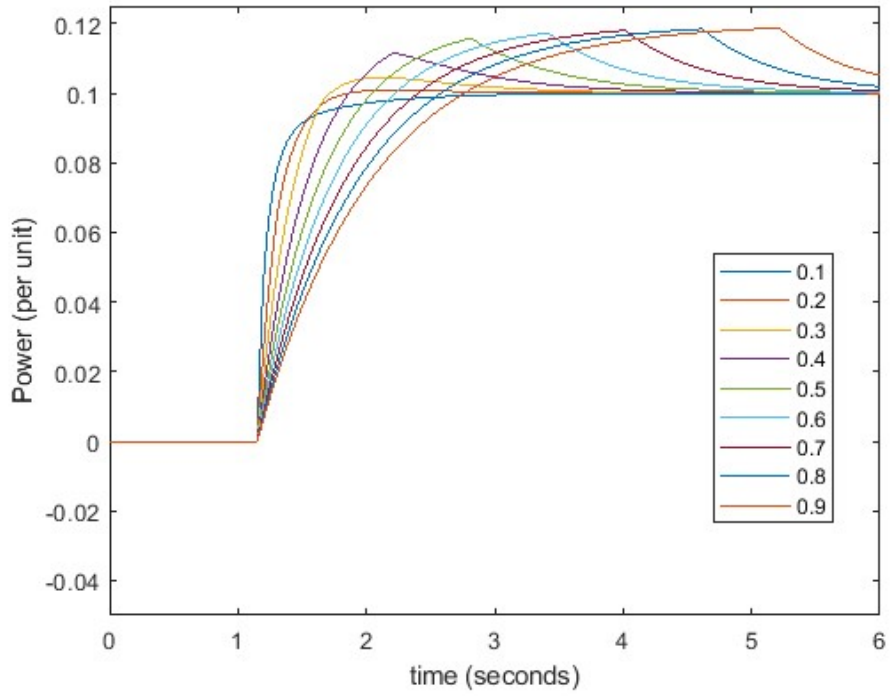

Figure 4.20: Overlaid VSG power outputs of a 20% overmatched VSG with combined control for different time constants. Delay time = 0.15.

Next, the delay time is fixed at 0.15 while the ramp time constant is varied. The results of that experiment are shown in Figures 4.19 and 4.20. Figure 4.19 shows that the frequency is more forgiving of the ramp than the delay. A delay time of 0.7 and a time constant of 0.15 caused the frequency to dip below 59.3 Hz in Figure 4.16. In contrast, a delay time of 0.15 with a time constant of 0.7 kept the frequency above 59.3 Hz in Figure 4.19. The reason that a larger time constant is more tolerable than a longer delay is that even a little bit of VSG power has a positive impact on the ROCOF, far better than having no power injected at all. Figure 4.20 shows that a shorter time constant reduces the VSG's peak power. This is because a larger time constant increases the time it takes for the VSG to match the disturbance, allowing the frequency deviation to grow more. This increases the power command from primary frequency control, leading to the observable trend of power rising further for longer time constants. This is similar to the trend in Figure 4.17 where a longer delay also causes the VSG power to rise. However, the

time constant affects the shape of the rampup differently than the delay. Figure 4.17 shows that long delays lead to faster, steeper rampups but only up to a certain point. As explained earlier, when the initial power command reaches the VSG's nominal limits, the VSG does its best to ramp up power as fast as it can. In contrast, Figure 4.20 shows that a larger time constant leads to a more gradual power ramp, which makes sense. As with the delay, a longer ramp time is costly because it requires more energy and power capacity from the VSG. Larger delay and ramp times also lower the nadir frequency and delay the onset of steady-state, which is detrimental to the recovery process.

5. Summary and Conclusion

Interest in the health of the environment and concern over the depletion of fossil fuel reserves is driving worldwide interest in renewable energy sources like wind and solar. These energy sources are abundant and inexhaustible, but integrating them into the grid is a challenge. The grid was not designed to cope with large numbers of intermittent, converter-coupled generators. These types of generators degrade system stability by displacing traditional synchronous generators. In doing so, they also displace the stabilizing services those synchronous generators provide. The first stabilizing service is provided by the inertia of the generator's rotating mass. The inertia resists changes in frequency caused by a generation-load imbalance, thereby reducing the frequency's rate of change. Reducing the ROCOF reduces the risk of triggering anti-islanding relays and also delays the frequency nadir. The inertia response happens immediately and automatically. No human or computer intervention is required. Rather, the inertia response happens as a manifestation of Newton's first law of motion. The inertia response acts as a stop-gap measure to delay catastrophe. The inertia cannot resolve a disturbance on its own. That has traditionally been the job of the synchronous generator's governor. The governor monitors the speed of the generator and changes the mechanical power setpoint by an amount proportional to the frequency deviation. Unlike the inertia, the governor is a control system with delays so it does not immediately react to the disturbance. The combined efforts of inertia and governor response stabilize the frequency sometime after the disturbance. Displacing these two services makes the grid more vulnerable to disturbances.

Virtual synchronous generators offer a way to partially make up for the loss of traditional synchronous generators. The idea is to control a power converter in a way that mimics the inertia and governor response. In a VSG, the inertia response is emulated by derivative control and the

governor response (called “primary frequency control” in this thesis) is emulated by proportional control. The virtual synchronous generator is not a true generator because it does not transform any form of energy into electrical energy. Rather, it takes electrical energy that already exists and manipulates it with a power converter. The energy can come from generators or energy storage systems, but not all energy sources are equal. VSGs supplied by wind and solar generators are at the mercy of the weather. VSGs supplied by slow-ramping sources will be sluggish. When searching for an energy source to use with a VSG, important qualities to look for are affordability, reliability, and speed. Batteries score high on all three. Battery technology is well-developed and has been proven in the field.

An important disclaimer to make is that VSGs cannot completely replace synchronous generators. It would be wise for a grid operator to hold onto some synchronous generators. They are still the best source for supplying base load because they can generate a certain amount of power indefinitely, something which BESSs and RES generators cannot be relied on to do. Besides, not all synchronous generators are bad for the environment. Hydro, nuclear, and geothermal powerplants produce clean energy and do not burn fossil fuels. Since VSGs are a control system, they cannot immediately react to a disturbance the way that synchronous inertia does. A certain amount of synchronous inertia should be kept on the grid to buy enough time for a VSG to act. The minimum inertia required can be calculated from the swing equation by knowing the maximum allowable ROCOF and the size of the disturbance that the operator plans to manage. Enough inertia should be provided so that the ROCOF immediately after a disturbance does not trip anti-islanding relays.

Assuming the relays have not tripped, the grid is in a race against time to arrest the frequency fall before load has to be shed. This has traditionally been the job of the governors on

synchronous generators. Having fewer synchronous generators on the grid means fewer governors. To make things worse, having less inertia on the grid makes the ROCOF larger for a given disturbance, which shortens the time to the frequency nadir. Governors can need tens of seconds to respond, and that may be too long to wait if a particularly large disturbance occurs while the inertia is low. This is especially true of small power systems because they are inherently more susceptible to large disturbances. However, even large power systems can be vulnerable if their inertia falls low enough. Battery storage technology offers a solution to this problem. A BESS can deliver its full power in well under a second, which is must faster than the typical governor can act. When power is delivered sooner, the frequency nadir is delayed and the frequency deviation is attenuated. Results show that a response time of 5 s or greater is too slow to prevent UFLS for any disturbance size larger than a few percent for typical inertia constants. This is fine for large grids where the loss of a generator represents a relatively small disturbance, but not for smaller grids with fewer resources. Simulations of inertia response show how responding early can help prevent UFLS and make the grid more tolerant of low inertia. A response time under 500 ms is fast enough to be effective at preventing UFLS, and the BESS technology available today is capable of providing that performance.

An advantage of the VSG over the synchronous generator is that it can deliver its primary frequency control much faster than a governor can. The VSG can deliver its primary frequency control at the same time it delivers its inertia control, and there are advantages to doing so. Operating either inertia control or primary frequency control yields inferior performance control compared to the combination of the two. Each control has qualities that the other lacks. Inertia control starts off strong because the magnitude of the ROCOF is greatest in the immediate aftermath of the disturbance. However, the inertia control does not command enough power to

cover the disturbance. Primary frequency control starts off weak because the frequency deviation starts off small. It grows over time until it matches the disturbance size or reaches the VSG's rated power. By combining the two, we get a VSG which starts off strong and gets stronger over time until the disturbance is matched or the power limit is reached. Overlaid frequency plots for the three VSG controls show that the combined control has the best overall performance. The second-best performance comes from primary frequency control. Inertia control has the worst performance of the three, but having inertia control is better than having no VSG at all.

In general, a more powerful VSG is a more effective VSG in that it raises the nadir frequency and reduces the time it takes to reach steady-state. In order for a VSG to be capable of bringing the frequency to steady-state, it must be powerful enough to at least match the size of the disturbance. Even if the VSG cannot match the disturbance, its presence still benefits the grid. By injecting its full power into the grid, an undermatched VSG can effectively reduce the size of the disturbance. If the VSG can match the disturbance, then it must include primary frequency control if it is to bring the frequency to steady-state. On its own, inertia control does not bring the frequency to steady-state. Although primary frequency control can stabilize the frequency on its own, having inertia control does improve overall performance. Inertia control plays a supporting role. It is much more effective to strengthen the primary frequency control than the inertia control. Having an inertia control constant that's too high, relative to the size of the disturbance, can destabilize the VSG's control system.

This thesis concludes that BESS-based VSGs are an effective and practical way to provide frequency support services and recommends that they be included in plans to increase renewable energy generation.

References

[1] A. Ulbrig, T.S. Borsche, and G. Andersson, "Analyzing rotational inertia, grid topology and their role for power system stability," *IFAC-PapersOnLine*, vol. 48, no. 30, pp. 541-547, 2015.

[2] A. Ulbrig, T.S Borsche, and G. Andersson, "Impact of low rotational inertia on power system stability and operation," *IFAC Proceedings Volumes*, vol. 19, no. 3, pp. 7290-7297, Aug. 2014.

[3] M. Dreidy, H. Mokhlis, and S. Mekhlief, "Inertia response and frequency control techniques for renewable energy sources: a review," *Renewable and Sustainable Energy Review*, vol. 69, pp. 144-155, March 2017.

[4] R. Shah, N. Mithulananthan, R.C. Bansal, and V.K. Ramachandaramurthy, "A review of key power system stability challenges for large-scale PV integration," *Renewable and Sustainable Energy Review*, vol. 41, pp. 1423-1436, Jan 2015.

[5] E. Muljadi, V. Gevorgian, M. Singh, and S. Santosa, "Understanding inertial and frequency response of wind power plants," in *IEEE Symposium on Power Electronics and Machines in Wind Applications*, 2012, pp. 1-8.

[6] P. Tielens, and D. Van Hertem, "The relevance of inertia in power systems," *Renewable and Sustainable Energy Reviews*, vol. 55, pp. 999-1009, March 2016.

[7] J.J. Grainger, and W.D. Stevenson, *Power Systems Analysis*. McGraw-Hill, 1994.

[8] P. Sauer, M. Pai, and J. Chow, *Power System Dynamics and Stability with Synchrophasor Measurement and Power System Toolbox*. Wiley, 2017.

[9] M.P.N. van Wesenbeeck, S.W.H. de Haan, P. Varela, and K. Visscher, "Grid tied converter with virtual kinetic storage," in *2009 IEEE Bucharest PowerTech Conference*, 2009, pp. 1-7.

[10] N.W. Miller, K. Clark, and M. Shao, "Frequency responsive wind plant controls: impacts on grid performance," in *Proceedings of the 2011 IEEE Power and Energy Society General Meeting*, 2011, pp. 1-8,

[11] GE Energy. "Western Wind and Solar Integration Study: February 2008-February 2010," NREL Report. No. SR-550-47434. May 2010.

[12] P.V. Brogan, R.J. Best, D.J. Morrow, K. McKinley, and M.L. Kubrik, "Effect of BESS response on frequency and ROCOF during underfrequency transients*," IEEE Transactions on Power Systems*, vol. 34, no. 1, pp. 575-583, Jan. 2019.

[13] H. Bevrani and J. Raisch, "On virtual inertia application in power grid frequency control," *Energy Procedia*, vol. 141, pp. 681-688, Dec 2017.

[14] M. Torres and L. Lopes, "Virtual synchronous generator control in autonomous wind-diesel power systems," in *Proceedings of the IEEE Electrical Power and Energy Conference*, 2009, pp. 1-6.

[15] V. Karapanos, S. de Haan, and K. Zwetsloot, "Real time simulation of a power system with VSG hardware in the loop," in *Proceedings of the 37th Annual Conference of the IEEE Industrial Electronics Society*, 2011, pp. 3748 – 3754.

[16] A. Vassilakis, P. Kotsampopoulos, N. Hatziargyriou, and V. Karapanos, "A battery energy storage based virtual synchronous generator," in *Bulk Power System Dynamics and Control -IX Optimization, Security, and Control of the Emerging Power Grid (IREP)* 2013, pp.1-6.

[17] H.-J. Moon, A.-Y. Yun, E.-S. Kim, and S.-l. Moon, "An analysis of energy storage systems for primary frequency control of power systems in South Korea," *Energy Procedia*, vol. 107, pp. 116-121, Feb. 2017.

[18] S.M. Alhejaj and F.M. Gonzales-Longatt, "Impact of inertia emulation control of grid-scale BESS on power system frequency response," in *2016 International Conference for Students on Applied Engineering (ICSAE)*, 2016, pp. 254-258.

[19] J. Alipoor. Y. Miura, and T. Ise, "Distributed generation grid integration using virtual synchronous generator with adoptive virtual inertia," *in 2013 IEEE Energy Conversion Congress and Exposition*, 2013, pp. 4546-4552.

[20] F. Arrigo et al. "On the virtual inertia provision by BESS in low inertia power system," in *2018 IEEE International Energy Conference (ENERGYCON)*, 2018, pp. 1-6.

[21] K. Visscher and S.W.H. de Haan, "Virtual synchronous machines for frequency stabilization in future grids with a significant share of decentralized generation," in *CIRCED Seminar 2008: SmartGrids for Distribution*, 2008, pp. 1-4.

[22] A. Oudalov, D. Chartouni, and C. Ohler, "Optimizing a battery energy storage system for primary frequency control," *IEEE Transactions on Power Systems*, vol. 22, no. 3, pp. 1259-1266, Aug. 2017.

[23] A. Oudalov, D. Chartouni, C. Ohler, and G. Linhofer, "Value analysis of battery energy storage applications in power systems," in *2006 IEEE PES Power Systems Conference and Exposition*, 2006, pp. 2206 – 2211.

[24] S. Alhejaj and F. Gonzales-Longatt, "Investigation on grid-scale BESS on power system frequency response," in *2016 IEEE International Conference on Power system Technology (POWERCON)*, 2016, pp. 1-6.

[25] X.-Z. Yang, J.-H. Su, M. Ding, J.-W. Li, and D. Yan, "Control strategy for virtual synchronous generator in microgrid," in *4th Int. Conference on Electric Utility Deregulation and Restructuring and Power Technologies (DRPT),* 2011, pp. 1633-1637.

[26] J. Alipoor, Y. Miura, and T. Ise, "Power system stabilization using virtual synchronous generator with alternating moment of inertia," *IEEE Journal of Emerging and Selected Topics in Power Electronics*, vol. 3, no. 2, pp. 451-458, June 2015.

[27] X. Tan, Q. Li, and H. Wang, "Advances and trends of energy storage technology in microgrid*," International Journal of Electrical Power & Energy Systems*, vol. 44, no. 1, pp. 179-191, Jan. 2013.

[28] D.M. Greenwood, K.Y. Lim, C. Patsios. P.F. Lyons, Y.S. Lim, and P.C. Taylor, "Frequency response services designed for energy storage," *Applied Energy*, vol. 203, pp. 115-127, Oct. 2017.

[29] P.V. Brogan, R. Best, D.J. Morrow, C. Bradley, M. Rafferty, and M.L. Kubrik, "Triggering BESS inertia response with synchronous machine measurements," in *2018 IEEE Power & Energy Society General Meeting (PESGM)*, 2018, pp. 1-5.

[30] L.H. Walker, "10 MW GTO converter for battery peaking service*," IEEE Transactions on Industry Applications*, vol. 26, no.1, pp. 63-72, Jan/Feb 1990.

[31] T. Senjyu, T. Nakaji, K. Uezato, and T. Funabashi, "A hybrid power system using alternative energy facilities in isolated island," *IEEE Transactions on Energy Conversion*, vol. 20, no. 2, pp. 406-414, Oct. 2002.

[32] D. Kottick, M. Blau, and D. Edelstein, "Battery energy storage for frequency regulation in an island power system," *IEEE Transactions on Energy Conversion*, vol. 8, no. 3, pp. 455-459, Sep. 1993.

[33] G. Delille, B. Francois, and G. Malarange, "Dynamic frequency control support: A virtual inertia provided by distributed energy storage to isolated power systems," in *Innovative Smart Grid Technologies Conference Europe (ISGT Europe)*, 2010, pp. 1-8.

[34] T. Feehally et al., "Battery energy storage systems for the electricity grid: U.K research facilities," *in 8th IET International Conference on Power Electronics, Machines, and Drives (PEMD 2016)*, 2016, pp. 1-6.

[35] T. Overbye, J. Glover, and M. Sarma, *Power System Analysis and Design*, 6th Edition, Cengage Learning, 2015.

[36] N. Miller, C. Loutan, M. Shao, and K. Clark, "Emergency Response," *IEEE Power & Energy Magazine*, Nov/Dec 2013.

[37] V. Gevorgian, Y. Zhang, and E. Ela, "Investigating the impact of wind generation penetration in interconnection frequency response," *IEEE Transaction on Sustainable Energy*, vol. 6, no. 3, July 2015.

[38] J. Undill, "Primary frequency response and control of power system frequency," Lawrence Berkeley National Laboratory, Energy Analysis and Environmental Impacts Division. Feb. 2018.

[39] "Underfrequency load shedding 2006 assessment and review," ERCOT, Dec 18, 2006.

[40] R. Yan, T. Saha, N. Modi, N. Mosood, and M. Mosadeghy, "The combined effect of high penetration of wind and PV on power system frequency response," *Applied Energy*, vol. 145, pp. 320-330, May 2015.

[41] K.B. Samarkan, "Use of Smart Meters for Frequency and Voltage Control," Ph.D. Thesis, Cardiff University, 2012

[42] T. Borsche, A. Ulbrig, M. Koller, and G. Andersson, "Power and energy capacity requirements of storages providing frequency control reserves," in *IEEE PES General Meeting*, 2013, pp. 1-5.

[43] H. He, R. Xiong, and J. Fan, "Evaluation of lithium-ion battery equivalent circuit models for state of charge estimation by an experimental approach," *Energies*, vol. 4, pp. 582-598, March 2011.

Appendix A: Chapter 3 Main Code

```
clc
%frequency dynamics simulation of a SG and real power load
%chapter 3 program
%{
This simulation uses the classical model of a synchronous generator
with a infinite bus that consumes 1 pu of real power at the start
with unity power factor. This simulation examines the inertial response
of the synchronous generator resulting from various sudden changes in load
Governor and voltage controls are not modelled here
%}
%{
This script in particular is used to record the frequencies at different
times following different sized disturbances. This script is run for
different values of H.
%}

%Times are in seconds
timestep = .000001;
time = 0;
totalruntime = 1.1; %modify runtime to capture frequency at different T
disturbancetime = 1;

%The number represents the percent change in load disturbance
w05 = 2*pi*60;
w10 = 2*pi*60;
w15 = 2*pi*60;
w20 = 2*pi*60;
w25 = 2*pi*60;
w30 = 2*pi*60;
w35 = 2*pi*60;
w40 = 2*pi*60;
w45 = 2*pi*60;
w50 = 2*pi*60;

Pm = 1; %per unit power. Matches load of 1pu at the start

Pe05 = 1;
Pe10 = 1;
Pe15 = 1;
Pe20 = 1;
Pe25 = 1;
Pe30 = 1;
Pe35 = 1;
Pe40 = 1;
```

```
Pe45 = 1;
Pe50 = 1;

%Define constants
ws = 2*pi*60;
H =10;

%intantiate arrays to plot frequency
elements = int32(totalruntime/timestep);
f_array05 = zeros(elements,1);
f_array10 = zeros(elements,1);
f_array15 = zeros(elements,1);
f_array20 = zeros(elements,1);
f_array25 = zeros(elements,1);
f_array30 = zeros(elements,1);
f_array35 = zeros(elements,1);
f_array40 = zeros(elements,1);
f_array45 = zeros(elements,1);
f_array50 = zeros(elements,1);

timevector = zeros(elements,1);

index = 1; %starting index initialized

while(time<totalruntime)
if(time <disturbancetime)
    Pe05 = 1;
    Pe10 = 1;
    Pe15 = 1;
    Pe20 = 1;
    Pe25 = 1;
    Pe30 = 1;
    Pe35 = 1;
    Pe40 = 1;
    Pe45 = 1;
    Pe50 = 1;
else %At this point, the load suddenly changes,
    Pe05 = 1.05;
    Pe10 = 1.10;
    Pe15 = 1.15;
    Pe20 = 1.20;
    Pe25 = 1.25;
    Pe30 = 1.30;
    Pe35 = 1.35;
    Pe40 = 1.40;
    Pe45 = 1.45;
```

```
    Pe50 = 1.50;
end
    %Take a forward Euler step
    w_new05 = w05 + (ws/(2*H))*(Pm - Pe05)*timestep;
    w_new10 = w10 + (ws/(2*H))*(Pm - Pe10)*timestep;
    w_new15 = w15 + (ws/(2*H))*(Pm - Pe15)*timestep;
    w_new20 = w20 + (ws/(2*H))*(Pm - Pe20)*timestep;
    w_new25 = w25 + (ws/(2*H))*(Pm - Pe25)*timestep;
    w_new30 = w30 + (ws/(2*H))*(Pm - Pe30)*timestep;
    w_new35 = w35 + (ws/(2*H))*(Pm - Pe35)*timestep;
    w_new40 = w40 + (ws/(2*H))*(Pm - Pe40)*timestep;
    w_new45 = w45 + (ws/(2*H))*(Pm - Pe45)*timestep;
    w_new50 = w50 + (ws/(2*H))*(Pm - Pe50)*timestep;

    w05 = w_new05;
    w10 = w_new10;
    w15 = w_new15;
    w20 = w_new20;
    w25 = w_new25;
    w30 = w_new30;
    w35 = w_new35;
    w40 = w_new40;
    w45 = w_new45;
    w50 = w_new50;

    %convert to Hertz
    f_array05(index) = w05/(2*pi);
    f_array10(index) = w10/(2*pi);
    f_array15(index) = w15/(2*pi);
    f_array20(index) = w20/(2*pi);
    f_array25(index) = w25/(2*pi);
    f_array30(index) = w30/(2*pi);
    f_array35(index) = w35/(2*pi);
    f_array40(index) = w40/(2*pi);
    f_array45(index) = w45/(2*pi);
    f_array50(index) = w50/(2*pi);

    timevector(index) = time;

    time = time + timestep;
    index = index + 1;

end

%print the end frequencies
```

```
    f05 = f_array05(index-1);
    f10 = f_array10(index-1);
    f15 = f_array15(index-1);
    f20 = f_array20(index-1);
    f25 = f_array25(index-1);
    f30 = f_array30(index-1);
    f35 = f_array35(index-1);
    f40 = f_array40(index-1);
    f45 = f_array45(index-1);
    f50 = f_array50(index-1);

%Print the ROCOF
rocof05 = (f_array05(index-1) - f_array05(index-2))/timestep;
rocof10 = (f_array10(index-1) - f_array10(index-2))/timestep;
rocof15 = (f_array15(index-1) - f_array15(index-2))/timestep;
rocof20 = (f_array20(index-1) - f_array20(index-2))/timestep;
rocof25 = (f_array25(index-1) - f_array25(index-2))/timestep;
rocof30 = (f_array30(index-1) - f_array30(index-2))/timestep;
rocof35 = (f_array35(index-1) - f_array35(index-2))/timestep;
rocof40 = (f_array40(index-1) - f_array40(index-2))/timestep;
rocof45 = (f_array45(index-1) - f_array45(index-2))/timestep;
rocof50 = (f_array50(index-1) - f_array50(index-2))/timestep;
```

Appendix B: Chapter 4 Main Code

```
clc
close all
%Chapter 4
%{
This program builds on the model used for chapter 3 and adds a VSG.
The object of this program is to overlay the frequency response from the
4 control cases discussed. These are
1)base case (no VSG control)
2)inertia emulation only
3)primary frequency control only
4)combined inertia emulation and primary frequency control
%}

%Times are in seconds
timestep = .00001;
time = 0;
totalruntime = 6; %modify runtime to capture frequency at different T
disturbancetime = 1;

%the  digit represents the control case
w1 = 2*pi*60; %base case
w2 = 2*pi*60; %inertia emulation case
w3 = 2*pi*60; %PFC casae
w4 = 2*pi*60; %inertia emulation + PFC case

%Initialize power variables. Everything starts balanced
Pload = 1; %steady state initial load
Pm = 1;     %treated as a constant
Pe1 = 1;
Pe2 = 1;
Pe3 = 1;
Pe4 = 1;
%VSGs are not intially active
Pvsg1 = 0;
Pvsg2 = 0;
Pvsg3 = 0;
Pvsg4 = 0;
%initialize ROCOF estimation variables for the VSGs
ROCOF2 = 0;
ROCOF4 = 0;

%Define constants
ws = 2*pi*60; %nominal frequency
H = 3; %vary H for different results
```

```
%disturbance size and system limits
disturbance_size = 0.1;
ROCOF_max = 2*pi; %1 hertz
delta_w_max = 2*pi*0.7;

%VSG parameters
VSG_nominal_power = disturbance_size*1.2;
%kd = -VSG_nominal_power/ROCOF_max;
kd = -disturbance_size/ROCOF_max;
kp = (-VSG_nominal_power/delta_w_max)*2;
%kp = (-VSG_nominal_power/delta_w_max);

%VSG response times
Tvsg_delay = 0.15; %how long the VSG takes to respond to the disturbance
Tvsg_ramp = 0.15; %the time constant for the VSG to ramp up

%intantiate arrays to plot frequency, ROCOF and VSG power output
elements = int32(totalruntime/timestep);
f_array1 = zeros(elements,1);
f_array2 = zeros(elements,1);
f_array3 = zeros(elements,1);
f_array4 = zeros(elements,1);
rocof_array1 = zeros(elements,1); %in hertz
rocof_array2 = zeros(elements,1); %in hertz
rocof_array3 = zeros(elements,1); %in hertz
rocof_array4 = zeros(elements,1); %in hertz
vsg_array1 = zeros(elements,1);
vsg_array2 = zeros(elements,1);
vsg_array3 = zeros(elements,1);
vsg_array4 = zeros(elements,1);

timevector = zeros(elements,1);

index = 1; %starting index initialized

while(time<totalruntime)
   if(time <disturbancetime)
      Pload = Pm;
   else %At this point, the load suddenly changes,
      Pload = Pm + disturbance_size;
   end
   if(time >= disturbancetime + Tvsg_delay) %delay VSG activation
      Pvsg1 = 0;
      Pvsg2 = kd*ROCOF2; %case 2, inertia emulation only
      Pvsg3 = kp*(w3 - ws); %case 3, primary frequency control only
```

```
    Pvsg4 = kd*ROCOF4 + kp*(w4 - ws); %case 4, both inertia emulation and PFC

    %enforce nominal power limits on VSG2
    if(Pvsg2 > VSG_nominal_power)
        Pvsg2 = VSG_nominal_power;
    end
    if(Pvsg2 < -VSG_nominal_power)
        Pvsg2 = -VSG_nominal_power;
    end
    %enforce nominal power limits on VSG3
    if(Pvsg3 > VSG_nominal_power)
        Pvsg3 = VSG_nominal_power;
    end
    if(Pvsg3 < -VSG_nominal_power)
        Pvsg3 = -VSG_nominal_power;
    end
    %enforce nominal power limits on VSG4
    if(Pvsg4 > VSG_nominal_power)
        Pvsg4 = VSG_nominal_power;
    end
    if(Pvsg4 < -VSG_nominal_power)
        Pvsg4 = -VSG_nominal_power;
    end

    %ramp up
    Pvsg2 = (1-exp(-(time - (disturbancetime + Tvsg_delay))/Tvsg_ramp))*Pvsg2;
    Pvsg3 = (1-exp(-(time - (disturbancetime + Tvsg_delay))/Tvsg_ramp))*Pvsg3;
    Pvsg4 = (1-exp(-(time - (disturbancetime + Tvsg_delay))/Tvsg_ramp))*Pvsg4;
end

%record the VSG power output at each timestep
vsg_array1(index) = Pvsg1;
vsg_array2(index) = Pvsg2;
vsg_array3(index) = Pvsg3;
vsg_array4(index) = Pvsg4;

%VSG power displaces synchronous output power
Pe1 = Pload - Pvsg1;
Pe2 = Pload - Pvsg2;
Pe3 = Pload - Pvsg3;
Pe4 = Pload - Pvsg4;

%Take a forward Euler step
w1_new = w1 + (ws/(2*H))*(Pm - Pe1)*timestep;
w2_new = w2 + (ws/(2*H))*(Pm - Pe2)*timestep;
w3_new = w3 + (ws/(2*H))*(Pm - Pe3)*timestep;
```

```
    w4_new = w4 + (ws/(2*H))*(Pm - Pe4)*timestep;

    %calculate ROCOF estimates for the VSGs in rad/s^2
    ROCOF1 = (w1_new - w1)/timestep;
    ROCOF2 = (w2_new - w2)/timestep;
    ROCOF3 = (w3_new - w3)/timestep;
    ROCOF4 = (w4_new - w4)/timestep;

    %record the ROCOF in hertz/second at each timestep
    rocof_array1(index) = ROCOF1/(2*pi);
    rocof_array2(index) = ROCOF2/(2*pi);
    rocof_array3(index) = ROCOF3/(2*pi);
    rocof_array4(index) = ROCOF4/(2*pi);

    w1 = w1_new;
    w2 = w2_new;
    w3 = w3_new;
    w4 = w4_new;

    %record the frequency in Hertz at each timestep
    f_array1(index) = w1/(2*pi);
    f_array2(index) = w2/(2*pi);
    f_array3(index) = w3/(2*pi);
    f_array4(index) = w4/(2*pi);

    timevector(index) = time;

    time = time + timestep;
    index = index + 1;

end

%print the nadir frequencies
f1_nadir = min(f_array1);
f2_nadir = min(f_array2);
f3_nadir = min(f_array3);
f4_nadir = min(f_array4);

%Print the final ROCOF
rocof_end1 = rocof_array1(index-1);
rocof_end2 = rocof_array2(index-1);
rocof_end3 = rocof_array3(index-1);
rocof_end4 = rocof_array4(index-1);

%plot frequency response
figure
```

```
plot(timevector, f_array1)
%title('system frequency of the 4 VSG control cases (matched)')
xlabel('time (seconds)')
ylabel('frequency (Hz)')
ylim([59.2 60.1])
hold on
plot(timevector, f_array2)
plot(timevector, f_array3)
plot(timevector, f_array4)
legend('no inertia emulation or primary control','inertia emulation only','primary control
only','inertia emulation and primary control')

%plot ROCOF
figure
plot(timevector, rocof_array1)
%title('overlayed ROCOF over time of the 4 VSG control cases (matched)')
xlabel('time (seconds)')
ylabel('ROCOF (Hz/s)')
ylim([-1.1 0.2])
%ylim([-1.5 0.5])
hold on
plot(timevector, rocof_array2)
plot(timevector, rocof_array3)
plot(timevector, rocof_array4)
legend('no inertia emulation or primary control','inertia emulation only','primary control
only','inertia emulation and primary control')

%Plot VSG power
figure
plot(timevector, vsg_array1)
%title('overlayed VSG power over time of the 4 VSG control cases (matched)')
xlabel('time (seconds)')
ylabel('Power (per unit)')
ylim([-0.05 .125])
hold on
plot(timevector, vsg_array2)
plot(timevector, vsg_array3)
plot(timevector, vsg_array4)
legend('no inertia emulation or primary control','inertia emulation only','primary control
only','inertia emulation and primary control')
```